A PM_{10} EMISSION FACTOR FOR FREE STALL DAIRIES

A Thesis

by

LEE BARRY GOODRICH

Submitted to the Office of Graduate Studies of
Texas A&M University
in partial fulfillment of the requirements for the degree of

MASTER OF SCIENCE

May 2006

Major Subject: Biological and Agricultural Engineering

A PM_{10} EMISSION FACTOR FOR FREE STALL DAIRIES

A Thesis

by

LEE BARRY GOODRICH

Submitted to the Office of Graduate Studies of
Texas A&M University
in partial fulfillment of the requirements for the degree of

MASTER OF SCIENCE

Approved by:

Co-Chairs of Committee,	Calvin B. Parnell
	Saqib Mukhtar
Committee Member,	Michael A. Tomaszewski
Head of Department,	Gerald Riskowski

May 2006

Major Subject: Biological and Agricultural Engineering

ABSTRACT

A PM_{10} Emission Factor for Free Stall Dairies. (May 2006)

Lee Barry Goodrich, B.S., Texas A&M University

Co-Chairs of Advisory Committee: Dr. Calvin B. Parnell
Dr. Saqib Mukhtar

Ambient concentration measurements of total suspended particulate (TSP) were made at a commercial dairy in central Texas during the summers of 2002 and 2003. The facility consisted of both open pen housing and free-stall structures to accommodate approximately 1840 head of milking cattle. The field sampling results were used in the EPA approved dispersion model Industrial Source Complex Short Term version 3 (ISCST-v3) to estimate emission fluxes and ultimately a seasonally corrected emission factor for a free-stall dairy.

Ambient measurements of TSP concentrations for sampling periods ranging from 2 to 6 hours were recorded during the summer of 2002. The mean upwind concentration was 115μg/m^3 with a maximum of 231μg/m^3 and a minimum of 41.4μg/m^3. The mean net downwind TSP concentration was 134μg/m^3 with a maximum of 491μg/m^3 and a minimum of 14μg/m^3. Field sampling at this same dairy in the summer of 2003 yielded significantly more 2 to 6 hour TSP concentration measurements. The mean upwind TSP concentration was 76μg/m^3 with a maximum concentration of 154μg/m^3. The mean net

downwind TSP concentration was 118μg/m^3 with a maximum of 392μg/m^3 and a minimum of 30μg/m^3.

The particle size distributions (PSD) of the PM on the downwind TSP filters was determined using the Coulter Counter Multisizer. The results of this process was a representative dairy PM PSD with 28% of TSP emissions being PM_{10}.

The reported PM_{10} 24-hour emission factors were 4.7 kg/1000hd/day for the free-stall areas of the facility and 11.7 kg/1000hd/day for the open pen areas of the dairy. These emission factors were uncorrected for rainfall events. Corrections for seasonal dust suppression events were made for the San Joaquin Valley of California and the panhandle region of Texas. Using historical rainfall and ET data for central California, the seasonally corrected PM_{10} emission factor is 3.6kg/1000hd/day for the free-stalls, and 8.7kg/1000hd/day for the open pens. For Texas, the seasonally corrected emission factor is 3.7kg/1000hd/day for the free-stall areas and 9.2kg/1000hd/day for the open lot areas.

I dedicate this thesis to my wife and my family. Their continued support has encouraged me throughout this work and continues to do so each day.

ACKNOWLEDGEMENTS

I would like to thank my wife Andrea for her infinite understanding and tolerance of me throughout. Without her support I don't know if this ever would have been completed. I would also like to thank my committee, Dr. Parnell, Dr. Mukhtar, and Dr. Tomaszewski and the CAAQES faculty for the chance to attend graduate school. Their contribution to this work was invaluable. They provided me with direction and funding that allowed me to complete this work. The Crew's contribution to my work, whether it be at the dairy sampling, weighing filters, or prep work before the sampling trips, made conducting this research possible. All these people and many more were critical to me completing my research.

TABLE OF CONTENTS

Page

LIST OF FIGURES

FIGURE Page

LIST OF TABLES

TABLE Page

TABLE Page

CHAPTER I

INTRODUCTION

The agricultural industry is coming under increased scrutiny as a source of particulate matter less than a nominal 10 micrometers aerodynamic equivalent diameter (PM_{10}). This is especially true in PM_{10} non-attainment areas such as the San Joaquin Valley in California. State Air Pollution Regulatory Agencies (SAPRA's) are required to include in their respective State Implementation Plans (SIP), proposed methods and procedures to bring non-attainment areas into attainment within a time limit established by USEPA. The methods and procedures are impacted by annual PM_{10} emissions as defined by the respective state emissions inventories and allowable PM_{10} emission rates corresponding to permit conditions. Emissions inventories and emission rates are determined by SAPRAs using PM_{10} emission factors. The EPA publication referred to as AP-42 list a large number of PM_{10} emission factors. The process used by SAPRAs for bringing non-attainment areas into attainment is to reduce pollutant emissions at the source. The focus of the SIP is to reduce pollutant emission rates such that the public is not exposed to ambient concentrations exceeding the National Ambient Air Quality Standards (NAAQS). Many times, SAPRAs start with reducing emissions from the largest sources listed in the state's emissions inventory.

This thesis follows the style and format of the *Transactions of the ASABE*

Many agricultural sources do not have pollutant emission factors or the existing emission factor is not based upon sound science. For pollutant sources with no established emission factor, the SAPRA will look for emission factors in AP-42 for similar industries and assume that they can be used to determine emission rates for permitting and annual pollutant emissions for emission inventory purposes.
The dairy industry does not have an existing PM_{10} emission factor in AP-42. In the view of regulators in California, dairies are similar to cattle feed yards. The California SAPRA assumed the dairy PM_{10} emission factor could be calculated by from a discredited AP-42 TSP emission factor of for dairies was based on the AP-42 emission factor for cattle feed yards which incorrectly causes dairies to appear as a high priority target for PM_{10} reductions. The use of the former cattle feed yard emission factor is inappropriate!

Dairies and feed yards have significantly different housing environments suggesting that the feed yard emission factor is not applicable towards free stall dairies. For example, feed yards have all of their cattle in open pens on what is known as manure pack. The manure pack is dried feces from cattle that have been compacted by the weight of the cattle walking on top of it, which then forms a hard dry surface whenever there has been no precipitation. The action of the cattle moving around on the manure pack is the primary source of particulate matter (PM) emissions from feed yards. Conversely, free stall dairies will keep the lactating portion of their herd in free stall structures. These structures are typically open sided barns with paved flooring and flush lanes used for

manure removal. The cattle are free to roam around the structure and lie down in individual free stalls. The arrangement of a free stall facility can be seen in figure 1.

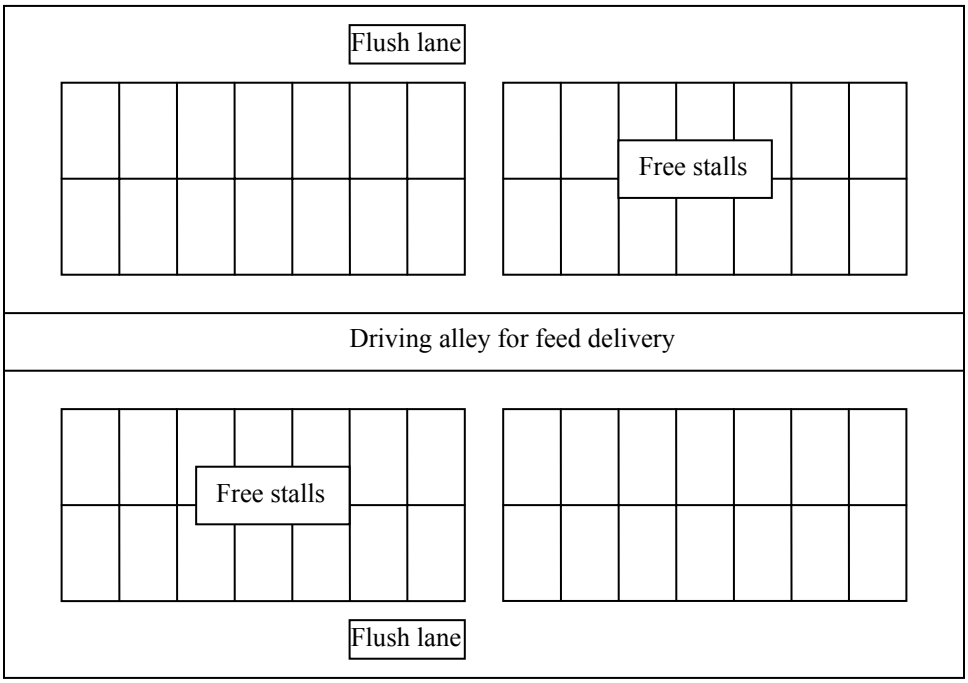

Figure 1. Schematic of a free stall dairy. The free stalls are individual bunks for cattle to lay in while resting and are filled with some sort of soft bedding material like composted manure or sand.

The flush lanes are located on each side of the free stalls and are the primary location for manure collection. These lanes are either flushed or scraped multiple times daily to remove the accumulated manure. The frequency of removal from this area prevents the manure from drying and becoming a source of PM emissions. The free stalls themselves are filled with various types of bedding material such as sand, wood chips or composted manure. The physical contact of the herd with the bedding material represents the only viable source of significant PM entrainment from the free stall structures. The open pens

are very similar to feed yard pens, but in contrast, have a much lower stocking density (~43 m^2/hd in dairies vs. ~14.0 m^2/hd in feed yards) and significantly less activity. The lower activity levels of dairy cattle are due to the fact that they are much larger animals, and that they are more accustomed to surrounding activity. Both factors lead to less movement in the pens.

The significant differences between feed yards and dairies demonstrate that applying any type of modified feed yard emission factor to a free stall dairy is totally inappropriate. In order to make future regulation of the dairy industry appropriate, it is imperative that a separate emission factor be developed that represents the actual conditions at free stall dairies, and that is applicable in the regulatory process.

The development of an appropriate emission factor for free-stall dairies is complicated by the lack of a standard method for determining emissions from ground level area sources (GLAS). Unlike most industrial sources such with smoke stacks such as power plants, GLAS emissions are not confined to a small uniform area of emissions. They are by definition spread over a large area and are highly variable. Therefore, the emissions from these sources must be measured indirectly. This is done by measuring a concentration of PM downwind of the source and using a dispersion model to determine the emission rate that must have produced that concentration. This process uses the source configuration and ambient meteorological conditions to describe the dispersion that occurs between the source and the sampler. There are many different methods for

determining the dispersion between the source and receptor. Two specific methods will be compared in this paper, Industrial Source Complex Short Term version 3 (ISC-STv3) and various versions of the fixed height box model.

CHAPTER II

RESEARCH OBJECTIVES

The goal of this research was to develop PM_{10} emission factors for dairies based upon sound science. One protocol selected for this project was to measure the net PM_{10} concentrations and back-calculate emission rates using the EPA approved ISC-STv3 model. It was hypothesized that a simpler protocol could be developed using the box model that would be equivalent to ISC-STv3. The results of both models would then be compared by developing an emission factor based on sampling data collected at a central Texas dairy. The two objectives of this research were as follows:

1. Analyze the feasibility of using the fixed height box model as a viable method for development of emission factors for fugitive sources of PM emitted by dairies.
2. Develop a PM_{10} emission factor for dairies using the EPA approved dispersion model, ISC-ST3.

CHAPTER III

LITERATURE REVIEW

In order to understand the impending problem with dairies, it is necessary to analyze the basis for the current emission factor and its development. Peters and Blackwood (1977) developed an emission factor of 127 kg/1000hd/day total suspended particulate matter (TSP) (280 lb/1000hd/day TSP) for feed yards using sampled PM concentration data reported by Algeo et al. (1972). The Algeo data represented the only fugitive PM emissions data available at the time. Although this AP-42 emission factor has been deleted from AP-42 by EPA, some states are continuing to use it in their permitting process for both dairies and feed yards. The use of this emission factor for dairies and feed yards dairies is inappropriate

Algeo et al. (1972) conducted ambient sampling upwind and downwind at 25 separate feed yards in California during the summer of 1971. The purpose of the work was to obtain data on the effectiveness of different control strategies for PM emissions that were being applied at the time. The data collected were not intended for use as the basis for a feed yard emission factor. However, these data were the basis for the AP-42 emission factor for cattle feed yards. The Peters and Blackwood unpublished study was funded by EPA.

Parnell, (1994) evaluated the methods used by Peters and Blackwood (1977) in an effort to update the emission factor using more recent and complete sampling data. She identified the following five limitations of the Peters and Blackwood study:

- The sampling was done only in California during the summer months, thus not representing any seasonal or regional variation in the measurements.
- The location of the samplers in relation to the source was not reported.
- The atmospheric conditions (wind speed, direction, shift, and stability class) were not reported.
- The utilization of emission control methods were not reported in the work done by Algeo et al. (1972).
- The sizes of the individual feed yards in the study were not reported by Algeo et al. (1972).

Taking all of these limitations into account Parnell, (1994) reported emission factors for feed yards by applying the Fugitive Dust Model (FDM) to sampling conducted by Sweeten et al. (1988). The emission factors reported by Parnell (1994) used significantly more data recorded at the time of sampling than Peters and Blackwood. All meteorological conditions were known, as well as the feed yard sizes, and cattle spacings.

Parnell (1994) discovered that EPA was planning to replace the area algorithm used in Industrial Source Complex version 2 (ISCST2) with the Fugitive Dust Model (FDM). She reported results based upon back-calculating emission rates using FDM.

The FDM algorithm divides the source into separate areas attributing the emissions from each area to a specific line source, and then uses the CALINE 3 line source algorithm (equations 1 & 2) to calculate the contribution of each line source to the receptor. The sum of all the line source concentrations is the resulting concentration at the receptor.

$$C_{10} = \frac{K}{2\pi\sigma_y}\int_{y_1}^{y_2} \exp\left(\frac{-y^2}{2\sigma_y^2}\right)dy \qquad (1)$$

where k is as follows:

$$K = \frac{q}{u\sigma_z}\left(\exp\left(-\frac{1}{2}\frac{(z-H)^2}{\sigma_z^2}\right)+\exp\left(-\frac{1}{2}\frac{(z+H)^2}{\sigma_z^2}\right)\right) \qquad (2)$$

where:

- C_{10} = concentration of pollutant ($\mu g/m^3$);
- y_1, y_2 = extent of line source;
- q = emission rate ($\mu g/m/s$);
- σ_y, σ_z = Pasquill-Gifford plume spread parameters based on stability class (m);
- u_s = average wind speed at pollutant release height (m/s);
- z = receptor height; and
- H = emission height.

Sweeten et al. (1988) reported measured TSP concentrations for three feed yards. The three feed yards had cattle populations, at the time of sampling, of 45,000, 42,000 and 17,000 head. Samplers were placed upwind and downwind of the facility during each sampling event. The mean, net, measured TSP concentration was 412±271 $\mu g/m^3$ TSP.

The work done by Sweeten and Parnell (1989) and Sweeten and et al. (1998) demonstrated that 25% of the TSP emitted from a feed yard was PM_{10} which was accepted by the EPA. The use of the actual sampler locations, feed yard sizes, spacing, and meteorological conditions yielded a final emission factor of 4.5 kg/1000hd/day TSP (Parnell, 1994), which is significantly less than the Peters and Blackwood emission factor of 127 kg/1000hd/day TSP. The Parnell (1994) emission factors represented emission factors developed using significantly more field data recorded at the time of sampling than Peters and Blackwood.

Subsequent work by Parnell et al.,(1999) reported additional evaluations on the Peters and Blackwood emission factor for cattle feed yards reported in AP-42. Peters and Blackwood (1977) used the Algio data to develop a TSP emission factor for cattle feed yards utilizing the infinite line source Gaussian dispersion modeling algorithm. Equation 3 is the equation for the infinite line source algorithm (Wark et al. 1998).

$$C_{10} = \frac{2Q_L 10^6}{\sqrt{2\pi}(\sigma_z u)} e^{\left(-\frac{1}{2}\left(\frac{H}{\sigma_z}\right)^2\right)} \quad (3)$$

where:

- C_{10} = steady state 10-minute concentration measured ‘x’ meters downwind of source;
- Q_L = emission rate (g/m/s);

- σ_z = vertical dispersion parameter, a function of downwind distance and atmospheric stability class;
- u = wind speed (m/s); and
- H = height of emissions (m).

Since many of the parameters required to estimate Q_L using equqtion 3 were not reported by Algeo et al. (1972), Peters and Blackwood (1977) assumed values. The following assumptions were made for all concentration measurements at each of the 25 feeyards:

- Wind speed was assumed to be 4.47 m/s.
- Stability class was assumed to be 'C'.
- The sampler location (x) was assumed to be 50 meters downwind of the source.
- The vertical spread parameter, σ_z, is a function of both stability class and downwind receptor location. For stability class C, a receptor located 50 meters downwind from the source will result in σ_z equaling 4 meters.
- They assumed that the emissions release height, H, was 3.05m. This assumption suggests that the cattle were floating in the air. It would seem more appropriate to assume thePM release height was at ground level (H=0m) with no plume rise.
- The size of the feed yards sampled by Algeo et al. (1972) were not reported.. Peters and Blackwood assumed that the all sampled feed yards averaged 8,000 head.
- The cattle spacing was assumed to be 13.9 square meters per head.

- Each feed yard was assumed to be perfect a square, making the modeled feed yard a 334 meter square area.

In order to use equation 3 in the development of a feed yard emission factor, Peters and Blackwood approximated the10-minute concentrations using the 24-hour TSP measured concentrations reported by Algeo et al. (1972) using the "power law" model (Wark et al. 1998) shown in equation 4.

$$C_{10} = C_{1440}\left(\frac{1440}{10}\right)^{0.17} \quad (4)$$

where:

- C_{10} = the estimated 10-minute concentration μg/m^3 and
- C_{1440} = the reported measured 24-hour (1440 minutes) concentrations.

The 10-minute average concentration is 2.33 times the 24-hour concentration.

Equation 5 is the result of substituting the assumed values for u, σ_z, and H into equation 3 and solving for Q_L. This equation would normally be used to determine an emission rate in grams per meter per second (mass per length per time). To obtain flux in units of mass per area per time, Peters and Blackwood divided Q_L by 330m (the width of the assumed square yard with 8000 head and a spacing of 13.9m^2/head). They ultimately reported their results in units of mass per 1000 head per day.

$$Q_L = 30 \bullet 10^{-6} C_{10} \quad (5)$$

Parnell et al. (1999) reported that there was a problem with equation 5. It was not the equation used by Peters and Blackwood (1977) to estimate Q_L from C_{10}. Equation 6 was used.

$$Q_L = 24.2 \bullet 10^{-6} C_{10} \quad (6)$$

Although equation 6 was used, the basis for it is unknown. Equation 7 is the resulting equation with the emission release height at ground level (H=0m).

$$Q_L = 22.4 \bullet 10^{-6} C_{10} \quad (7)$$

If equation 7 had been used by Peters and Blackwood, the resulting emission factor would have been 118 kg/1000hd/day TSP. Grelinger and Lapp (1996) reported that they had contacted Algeo and learned that the average number of head on the 25 sampled feed yards was 20,000 to 25,000 head in contrast to the 8,000 head assumed in their study. Using the revised estimates of feed yard size and emission height, the more correct emission factor with Algeo's data should have been 71 kg/1000hd/day TSP (Parnell et al., 1999).

Parnell et al. (1999) reported results for additional studies on PM emissions from feed yards. The concentration measurements consisted of 14 sampling periods using co-located TSP and PM_{10} samplers. Meteorological measurements for the sampling periods

were recorded. The Industrial Source Complex Short-Term version 3 (ISC-ST3) model was used to determine emission rates (factors) from the measured concentrations. This process consisted of back-calculating emission rates (fluxes) using the meteorological conditions corresponding to the conditions existing for each test. This process utilized ISC-ST3 which was EPA approved dispersion model most often used by regulatory agencies in the permitting process. Parnell et al. (1999) reported an average emission factor of 34 kg/1000hd/day TSP, uncorrected for seasonal variations. This was significantly lower than the original emission factor reported by Peters and Blackwood. Using the particle size distribution (PSD) reported by Sweeten et al. (1988, 1998) the resulting emission factor was reported as 8.6kg/1000hd/day.

Parnell et al. (1999) also developed methodology to approximate the zero PM emission days due to rainfall events. Effective rainfall amounts were determined, using the USDA NRCS curve number method, which corresponded to multiples of the local daily evapotranspiration. The probability of these events was then determined using historical rainfall records. Using this method, it was determined that approximately 77 days, or 21% of the time, there were no emissions from feed yards. This resulted in an annual corrected emission factor of 6.8kg/1000hd/day.

The numerous errors and shortcomings of the Peters and Blackwood PM emission factor for cattle feed yards lead the EPA to remove it from AP-42. Although the cattle feed yard AP-42 emission factor was removed from AP-42, it is still being used as the basis

for dairy emission factors in some states. For example, California used the former AP-42 TSP cattle feed yard emission factor as the basis for dairies. They used contractor data reported by Houck et al. (1989) suggesting that the PM_{10} fraction of TSP was 48.18%. This result was determined using Parallel Impactor Sampling Devices for 24-hour sampling intervals for a total of six samples at a central California dairy. Using the Peters and Blackwood TSP emission factor of 127 kg/1000hd/day and the PM_{10} mass fraction of 0.4818, the dairy PM_{10} was estimated to be 61.2 kg/1000hd/day PM_{10}

There are two significant problems with this method for determining PM_{10} mass fraction. First, the preseparators used probably have the same errors associated with them that Buser et al. (2001) described for the EPA approved samplers. Buser determined that a correctly operating EPA approved PM_{10} sampler may over-sampler by as much as 300% or more based on the ambient PSD. As the mass median diameter (MMD) of the ambient dust becomes larger than 10μm, the PM_{10} samplers over-sample by increasingly larger amounts. The reported PM_{10} fraction will be incorrect if the PM_{10} sampler used to determine the PSD was over-sampling due to a large ambient PSD. Second, the extended sampling period allows for significant wind variation. During a 24-hour time period, there will be a portion of time that the sampler is not downwind of the source.. It is likely that ambient PM present upwind from the dairy source will have a smaller MMD than the particulate matter being emitted from the source. Therefore, the particle size distribution associated with 24-hour PM sampling will be biased towards a smaller MMD. Meteorological data was not reported in the Houk study. The lack of

meteorological data and the inherent errors associated with PM_{10} samplers make the Houck PM_{10}/TSP mass ratio highly suspect.

Flocchini et al. (2001) developed a fixed height box model in order to determine emission factors from area sources. This method is a small scale version of the box model described by Arya (1999). The box model consists of a theoretical box placed around the source of interest. The pollutants of interest entering and exiting the box are accounted for, and it is assumed that there is no reaction of pollutants inside the box, allowing for the conservation of mass within the box. Therefore, the change in concentration between the upwind and downwind edge of the box can be solely attributed to the emission sources within the box. Flocchini et al. (2001) used this approach to determine emissions from field preparation operations such as discing, ripping, and floating. To use this model, concentration measurements were made at the upwind and downwind edges of the field representing the edges of the box. The net concentration was determined by subtracting the upwind concentration from the downwind concentration, and attributing that change to the activity within the field. The net concentration, along with average wind speed, was used to determine the net mass of pollutants emitted during the sampling period. The net mass was then divided by the area covered during the sampling period to determine flux. This represents a new approach that does not directly use dispersion modeling, and will allow for a second method to determine emission fluxes from area sources.

The combination of the deficiencies of the previous studies, and their lack of application to actual dairy environments, has left the door open for inappropriate regulation of dairies. First, the errors associated with the Peters and Blackwood emission factor make its use, even for feed yards, inappropriate. Second, the significant differences between the operational characteristics of dairies and feed yards make the application of any emission factor developed for feed yards unacceptable for use as a basis for dairy emission factors.

CHAPTER IV

MODEL COMPARISON

As previously stated, it is imperative that the emission factors used in the air pollution regulatory process be accurate. Emission factors for ground level area sources (GLAS) are derived from emission fluxes, which are emission rates of pollutants in units of mass per unit area per unit time ($\mu g/m^2$-s). SAPRAs use emission factors for multiple reasons. One use of emission factors is to estimate downwind concentrations using modeling, which are then compared to the National Ambient Air Quality Standards (NAAQS). They are also used for emission inventory purposes to determine the total emissions from an associated industry. If an emission factor is too high, resulting in an inaccurate emissions inventory, the resulting SAPRA actions can lead to costly and unnecessary installation of abatement measures. Conversely, if the emission factor is too low, the resulting public exposure can pose a significant health risk. Since the NAAQS were designed to protect the public health (Cooper and Alley, 2002), it is vitally important that the predicted concentrations do not significantly under-estimate concentrations.

Identification of an appropriate method to determine emission fluxes from area sources is essential if a sound emission factor is to be developed. The problem with determining PM fluxes from area sources is inability to directly measure the emissions. Most industrial emission factors are developed for point sources that can be measured directly at the point of emissions. Conversely, area source emissions, particularly from animal

feeding operations, are spread over several hundred acres or more. The large expanse of area necessitates the development of an indirect method of determining emission fluxes.

Methods

The estimate of the flux as determined by the box model will be evaluated based on the EPA approved dispersion model ISC-STv3. This model is currently used to predict pollutant concentrations for permitting processes, and has an area source algorithm in it. The box model is of interest due to its current use as a tool in the development of area source emission factors specifically for agriculture. It is desired to explore the conditions in which the fixed height box model will always produce a conservative estimate of flux in relation to ISC-STv3, and how the box model can be modified to improve its performance.

Box Model

Flocchini, et al. (2001) used a small scale modification of the box model to determine the flux of pollutants from area sources. Initially, Flocchini et al. (2001) proposed a single box height of 4 meters, with a uniform pollutant concentration on both the upwind and downwind ends of the box. The box was assumed to be the width of the downwind edge of the field (Figure 2). The primary limits to the use of this model are that the wind direction be plus or minus 45 degrees from the sampling axis and that the field be a rectangle.

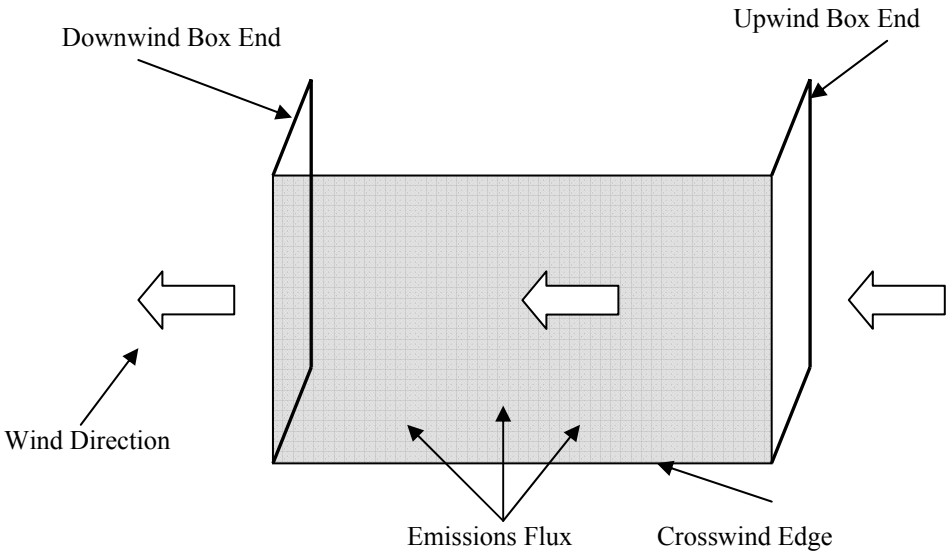

Figure 2. Schematic of box model algorithm. Emission fluxes are assumed to be uniform and constant over the GLAS surface. The concentrations at both the upwind and downwind edges of the source area assumed constant over the entire plane.

In order to calculate the flux, a simple mass balance is performed by calculating the mass flow rate of pollutant that enters the box and subtracting that from the mass flow rate of pollutant exiting the box. The emission flux is then calculated by dividing the total mass emission rate by the area of the emitting source (equation 8). It is assumed that the only air flow through the downwind edge of the box is due to the perpendicular component of the wind direction. This is the reason for the cosine (θ) function associated with the wind speed.

$$Q_A = \frac{W_B \bullet H \bullet C \bullet U \cos(\theta)}{W_S \bullet D} \qquad (8)$$

where:

- Q_A = emission flux ($\mu g/m^2$-s);
- W_B = width of box (m);
- H = height of box, 4 meters;
- U = average wind speed during sampling period (m/s)
- θ = deviation of wind direction from ideal;
- W_s = width of source;
- C = net measured concentration ($\mu g/m^3$); and
- D = field depth.

The box width is defined by the width of the source of interest. It is assumed that the concentrations measured at the upwind and downwind ends of the box are uniform in both the vertical and horizontal directions. Meister (2000) suggested that the vertical profile of pollutant downwind of an area source is better represented by a triangular distribution with a peak concentration occurring at approximately 25% of the total height of the plume and tapering down to zero at the top and bottom edge of the plume. Assuming the theoretical measured concentration is the maximum concentration, a triangular distribution will yield a flux that is ½ that of a uniform distribution of the same height. This is because the area of a triangle with the same base width (H) and peak concentration (C) as the uniform distribution has ½ the area of the square. To be conservative, our approach was to assume a uniform distribution. The height of the box is 4 meters, which also corresponds to a Pasquill-Gifford stability class 'C' vertical

dispersion parameter, σ_z, at 50 meters downwind from the source. Net concentration is determined by subtracting upwind sampler concentrations during the respective test periods from the downwind sampler concentrations.

The behavior of the box model in certain situations is of specific interest for this analysis. The interaction of the fixed box height and its relation to the upwind source depth is of interest due to the possibility of underestimating the total emissions. The reason for an assumed underestimation in this case is that as sources become larger in the upwind direction there is more likelihood that the plume shape in the vertical direction is not adequately described by a uniform 4 meter concentration. The behavior of the box model with varying wind directions is also of interest due to the simple handling of the varying wind direction by inserting the cosine(θ) term.

Industrial Source Complex Short-Term Version 3

ISC-STv3 is a steady state Gaussian plume model that can be used to predict downwind concentration from area sources (EPA, 1995a). ISC-STv3 is used to calculate 1-hour average concentrations at receptor locations placed anywhere around the source. The inputs for the model include the relative placement of sources and receptor locations, as well as meteorological conditions and emission fluxes. The equation that ISC-STv3 uses as the basis for all other calculations is a double Gaussian algorithm that represents a

point source (equation 9). This equation is then integrated in the crosswind direction to represent line sources as in equations five and six.

$$C = \frac{Q}{2\pi\, u \sigma_y \sigma_z} \exp\left[-\frac{y^2}{2\sigma_y^2}\right]\left\{\exp\left[-\frac{(H-z)^2}{2\sigma_z^2}\right] + \exp\left[-\frac{(H+z)^2}{2\sigma_z^2}\right]\right\} \qquad (9)$$

where:

- C = predicted concentration ($\mu g/m^3$);
- Q = emission rate ($\mu g/s$);
- u = wind speed at the point of emissions release (m/s);
- σ_y = Pasquill-Gifford horizontal plume spread parameter based on stability class (m);
- σ_z = Pasquill-Gifford vertical plume spread parameters based on stability class (m);
- H = height of plume release (m);
- y = crosswind distance from source to receptor (m); and
- z = height of receptor for concentration prediction (m).

Each of the inputs to ISC-STv3 are either measured in the field or are calculated from measured values in the field. The Pasquill-Gifford dispersion parameters are calculated based on the atmospheric stability class. The stability class is determined using wind speed and incoming solar radiation during the time of interest. These values are used in tables 1 and 2, along with the time of day to determine the stability class for a given modeling period.

Table 1. Key to solar radiation method for estimating daytime Pasquill-Gifford stability categories (EPA, 2000)

	Solar Radiation (W/m^2)			
Wind Speed (m/s)	≥925	925-675	675-175	<175
<2	1	1	2	4
2-3	1	2	3	4
3-5	2	2	3	4
5-6	3	3	4	4
≥6	3	4	4	4

Table 2. Key to cloudiness method for estimating nighttime Pasquill-Gifford (PG) stability categories (Turner, 1994).

	Night Cloudiness	
Wind Speed (m/s)	Cloudy (≥4/8)	Clear (≤3/8)
<2	5	6
2-3	5	6
3-5	4	5
5-6	4	4
≥6	4	4

The stability class is then used to determine the coefficients used to calculate the plume spread parameters using equations 10 and 11 for σ_y and σ_z respectively (Turner, 1994). Since the plume shape is assumed to be a normal distribution in both the vertical and horizontal planes, these equations represent the standard deviation of the plume in respective planes. For example, the σ_y calculation represents the standard deviation of the plume in the crosswind direction.

$$\sigma_y = \frac{1000 \bullet X \bullet \tan\left(C - D \bullet \ln\left(X\right)\right)}{2.15} \tag{10}$$

where:

- σ_y = Pasquill-Gifford horizontal plume spread parameter based on stability class (m);
- X = downwind distance from source to receptor (km); and
- C and D, are stability class specific constants.

$$\sigma_z = aX^b \tag{11}$$

where:

- σ_z = Pasquill-Gifford vertical plume spread parameter based on stability class (m);
- X = downwind distance from source to receptor (km); and
- a and b, are stability class specific constants.

The ISC-STv3 area source algorithm is similar to the algorithm used in Point Area and Line Sources 2.0 (PAL) (Peterson and Rumsey, 1987). The concentration is predicted by simulating the area source as a series of line sources that are perpendicular to the wind direction (Figure 3). In ISC-STv3 the orientation of source and receptor is defined according to the wind direction for the modeling period. The crosswind distance (Y) is the distance perpendicular to the wind direction from an emission point to a receptor. The downwind distance (X) is the distance from an emissions point to the receptor, parallel with the direction of the wind.

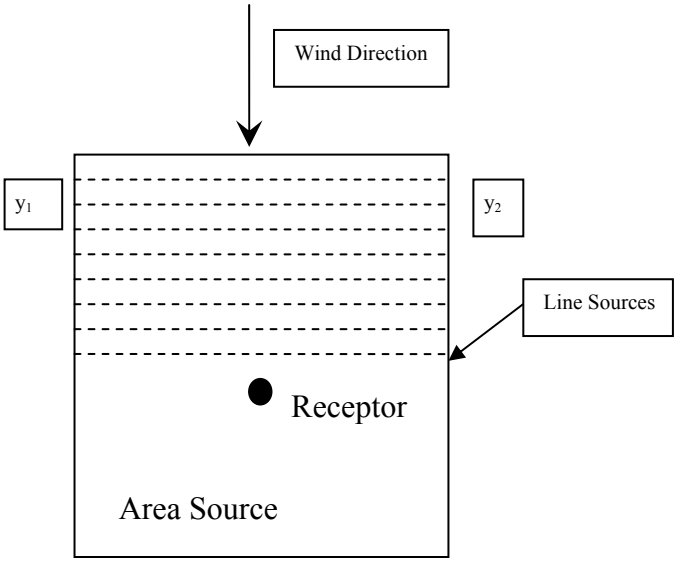

Figure 3. Schematic of ISC-STv3 area source algorithm. Dashed lines represent the line sources placed perpendicular to the prevailing wind, upwind of the receptor. The modeled concentration at the receptor is determined by summing the calculated concentration of each line source.

The number of line sources used is increased until the predicted concentration using N line sources converges with the predicted concentration using N-1 line sources. The only differences between ISC-STv3 and PAL are the method used for evaluation of equations 4 and 5, and the criteria used to determine convergence of the predicted concentration. These changes were made in order to optimize the computing time used to determine the concentration, but yield the same results (EPA, 1995b). ISC-STv3 can also handle more variations in the configuration of area sources. PAL limits area sources to strictly North-South East-West orientations (Petersen and Rumsey, 1987), while ISC-STv3 allows for any configuration of area sources. The method used by ISC-STv3 allows for the placement of receptors at any location in or around area sources. The only limitation on placement of receptors is the upwind distance to the nearest line source, which is due to the calculation of the σ_z parameter. When the upwind distance

from source to receptor approaches zero, σ_z approaches zero, yielding inconsistent results. Therefore, ISC-STv3 limits the minimum downwind distance, from source to receptor, to 1 meter.

In order to determine concentrations downwind of the source for varying wind directions ISC-STv3 effectively rotates the coordinates of the source and receptor to keep to that of the wind direction. This rotation maintains the ideal perpendicular orientation of wind direction and line source for all wind directions. Therefore, ISC-STv3 does not incorporate the change in wind direction into the Gaussian equation, but incorporates the change in wind direction before the Gaussian equation is used. This allows for much simpler calculations.

The evaluation of the area source algorithm is the result of the integration of equations 4 and 5. The integration is done numerically by using the infinite length line source model (equation 12), and then multiplying by a scalar to correct for edge effects (Turner, 1994). The effect of this calculation is that the area source closest to the receptor will have the largest effect on the total predicted concentration. As the distance from the receptor increases the relative contribution to the total concentration decreases. The decrease in concentration in the infinite length line source is attributed solely to the increased vertical dispersion of the plume with distance.

$$C = \frac{2q}{\sqrt{(2\pi)}\sigma_z u} \exp\left[-\frac{H^2}{2\sigma_z^2}\right] \qquad (12)$$

- where:
    - C = concentration of pollutant ($\mu g/m^3$);
    - y_1, y_2 = extent of line source;
    - q = emission rate ($\mu g/m/s$);
    - σ_z = Pasquill-Gifford vertical plume spread parameter based on stability class (m);
    - u_s = average wind speed at pollutant release height (m/s);
    - H = emission height.

The correction for edge effects is a function of the crosswind distance from the end of each line source, to the receptor (Y), and the horizontal plume spread parameter (σ_y). This is a different value for each line source in the model. Since the horizontal plume shape is represented by a normal distribution, equation 13 can be used to determine the fractional portion of the area under a normal curve. This value is used as a scalar to decrease the predicted concentration. Figure 4 is a graphical representation of the area where edge effects will occur.

$$S = \frac{Y}{\sigma_y} \tag{13}$$

where:

- S = number of standard deviations;
- Y = crosswind distance between receptor and edge of line source; and
- σ_y = horizontal plume spread standard deviation.

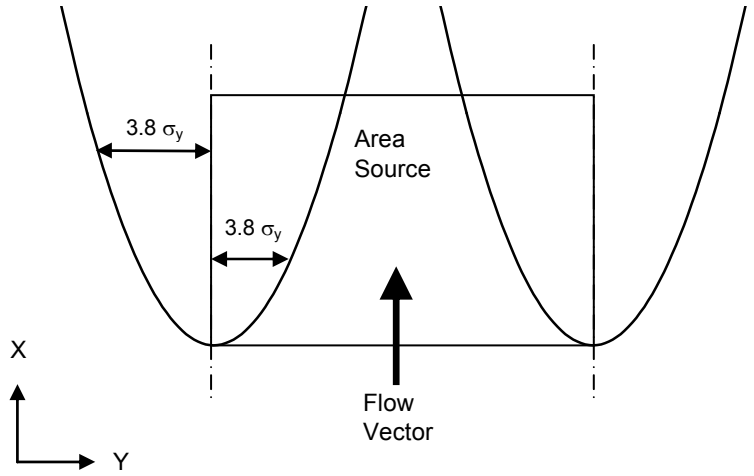

Figure 4. The region affected by the finite length line source algorithm in ISC-STv3. The region influenced by edge effects is within a distance of 3.8 σ_y from the end of any of the line sources.

Edge effects will occur anywhere within 3.8 σ_y of the edge of the line source. The magnitude of the edge effects can be demonstrated by looking at the profile of concentration versus horizontal location, in relation to the area source. Figure 5 shows the edge effects multiplier versus horizontal sampler location.

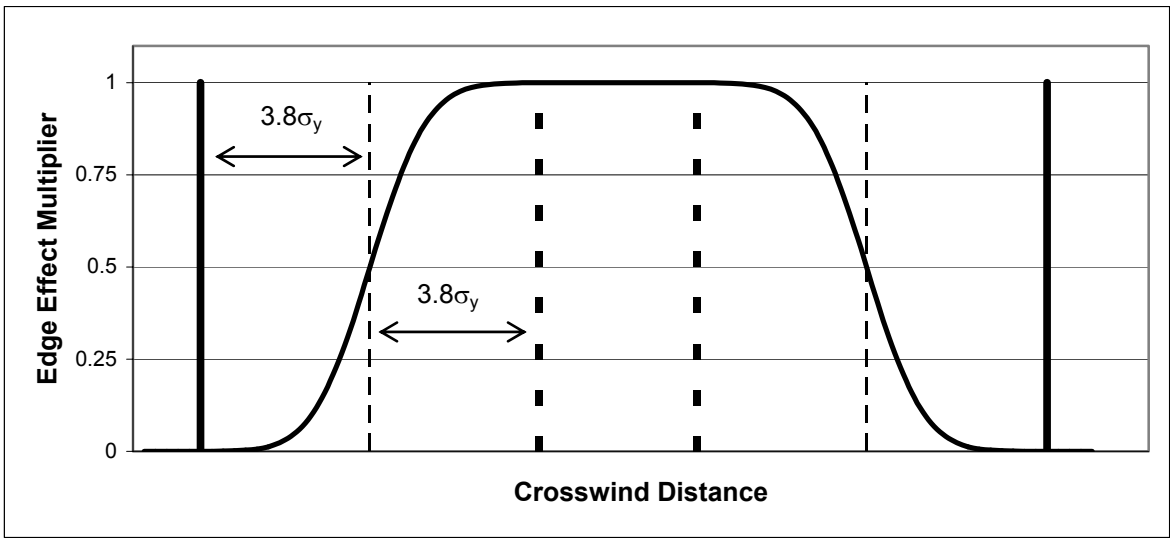

Figure 5. The magnitude of edge effects in the crosswind direction. The dashed lines represent a position directly downwind of the end of the line source. The peak concentration is reached at a distance of 3.8 σ_y towards the center of the field. There is no contribution to the concentration when the receptor is placed greater than a distance of 3.8 σ_y outside the edge of the field.

As the receptor location is moved from the centerline of the source towards the edge of the source, edge effects begin to influence the predicted concentration. Once the receptor location reaches a distance of 3.8 σ_y from the edge of the source, the predicted concentration will start to decrease and continue to do so until the predicted concentration becomes zero at a distance of 3.8σ_y from the edge of the field. It is important to note that the effect is observed independently for each line that is used to represent the source. Therefore, the lines that are closest to the receptor location will have a smaller relative width of the edge effects due to the smaller value of σ_y. The lines that are farther from the receptor will have a larger edge effect. This larger edge effect from line sources that are farther away is partially mitigated by the fact that the relative contribution of the line sources at greater distances decreases. The net effect of this is

that edge effects are only significant if the receptor is placed close to the crosswind edge of a source.

The final input used by ISC-STv3 is the mixing height. This is the top of the unstable layer near the ground. It represents the height at which the ambient temperature profile intersects with the dry adiabatic lapse rate. The equipment required to determine this value was not available, so the height was calculated using isopleths developed by Holzworth (1972). However, it is noted that mixing height will have little to no effect on the predicted concentration, if the source and receptor distances are small (EPA, 1987). Therefore, the only meteorological parameters that were varied in this analysis are wind direction, wind speed and stability class. All other parameters have no net effect on the results of the analysis.

Model Comparison

In order to evaluate the validity of the box model for large ground level area sources (GLAS) that may have emissions several hundred meters from the receptor, it is necessary to determine how the model will compare to an EPA approved dispersion model, namely ISC-STv3. This process involves determining an emission flux using the box model with a theoretical measured concentration, and then comparing the concentration predicted using ISC-STv3 and the box model predicted flux, to the nominally measured concentration. This was done for two types of area sources that are typically found on free stall dairies. First, a long narrow source that is similar to a free

stall structure on dairies, which for this analysis is configured in such as a way that the source is very wide. The second source configuration is that of a large square source similar to an open pen on a dairy. The actual dimensions of the sources vary depending on the analysis in order to determine the parameters of interest. The primary criterion of a large source is that it has significantly large depth, such that a small change in depth will not significantly affect the concentration prediction in ISC-STv3.

The box model was evaluated using ideal conditions, including a receptor placed in the middle of the downwind edge of the source, wind direction that is blowing directly from source to receptor, and one hour sampling periods. The final assumption made for this comparison was a constant nominal measured concentration of 200μg/m^3. These assumptions simplify equation 8 into equation 14.

$$Q_A = 800 \bullet \frac{U \cos(\theta)}{X} \tag{14}$$

where:

- Q_A = emission flux (μg/m^2/s);
- U = wind speed (m/s);
- θ = deviation of wind direction from ideal; and,
- X = field depth (m).

This equation allows for the variation of wind speed, stability class and wind direction in ISC-STv3. It is important to note that wind speed and flux are directly proportional, and

that flux and field size are inversely proportional. Therefore, a doubling of the wind speed will double the calculated flux, while a doubling of the field depth will decrease the flux by ½. This is also true in ISC-STv3. Therefore, the only meteorological parameters that affect this analysis are stability class and wind direction in ISC-STv3. Equation 14 represents that the source depth and emission flux are inversely proportional for a fixed measured concentration regardless of stability class. This relationship will lead the box model to predict an ever decreasing flux that is asymptotic to zero, as the source depth becomes larger. Figure 6 shows the relationship between the predicted flux and field depth for the box model and ISC-STv3. This plot was generated using a nominally measured concentration of 200 $\mu g/m^3$, ideal wind direction, and the receptor placed 1 meter outside the downwind edge of the source. It is clear that the fixed height box model is not conservative at all times for all stability classes. This is seen by the fact that there are situations in which the box model flux is higher than the ISC-STv3 predicted flux. In order to account for this problem, an effective depth will be developed for each stability class. The effective depth is the distance that the upwind fetch must be limited to, in order to ensure a conservative estimate from the box model. Figure 6 also shows that for all stability classes, as source depth becomes significantly large, there is little change in the ISC-STv3 predicted flux for a small change in source depth.

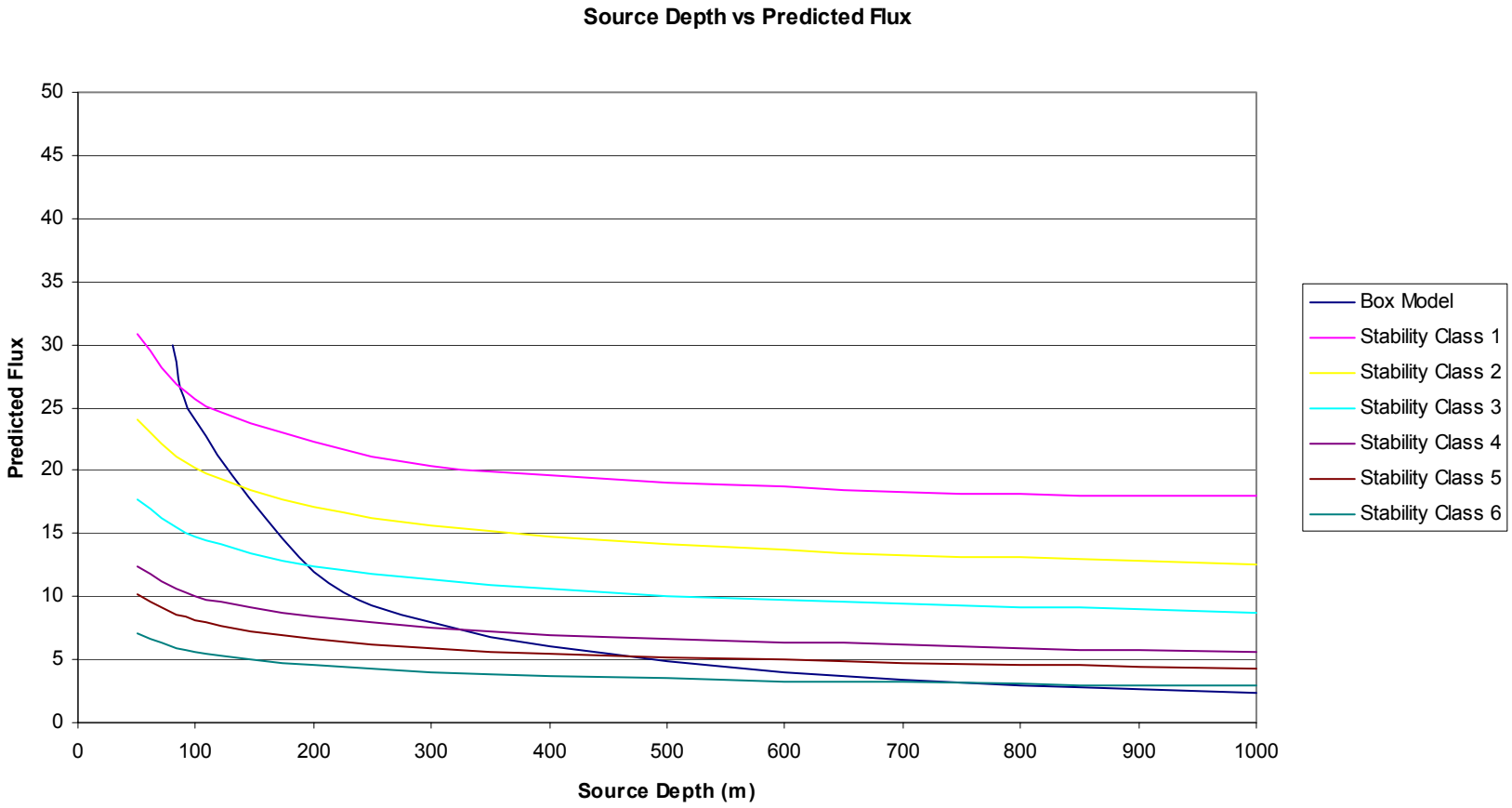

Figure 6. Relationship between source depth and predicted flux for both ISC-STv3 and the box model. The source is 1000 meters wide and varying depths.

Effective Field Depth

When using the box model to predict a flux, the assumption of a fixed height box leads to inconsistent results when compared to ISC-STv3. The assumption of a uniform concentration in a fixed height box is a representation of the actual plume that exists. The idea is to develop constraints where this remains to be a conservative estimate. In some cases, a uniform 4 meter plume height does not accurately characterize the entire plume height that is used in ISC-STv3. Some sources may be very large and have significant amounts of the plume that exceed the 4 meter height at the receptor location. This error is complicated by the fact that ISC-STv3 uses differing plume heights based on stability class for the same configuration. This can be seen in figure 6 by the distinctly different fluxes predicted for the same conditions while only changing stability class. The box height issue can be addressed by limiting the maximum source depth used in the box model, regardless of the actual depth of the source. This method will develop an effective depth that can be used to ensure the box model is a conservative estimate of flux compared to ISC-STv3, regardless of source dimensions.

The effective depth is defined as the depth at which ISC-STv3 predicts the same concentration as used in the box model to determine the emission flux. For example, using equation 14 with a 100 meter deep source and a wind speed of 4 m/s, the resulting emission flux is $32\mu g/m^2/s$. Using this flux in ISC-STv3 with a stability class of 'A' yields an ISC-STv3 predicted concentration of $182\mu g/m^3$. The ISC-STv3 predicted

concentration (182μg/m^3) is less than the theoretical measured concentration (200μg/m^3), making the estimation of flux too low using the box model. In order to increase the flux term for use in ISC-STv3, it is necessary to decrease the denominator in equation 14. By decreasing the field depth term in the box model, the same measured emissions are attributed to a smaller portion of the source, thus increasing the input flux for ISC-STv3. This process will then increase the ISC-STv3 predicted concentration. For example, by decreasing the effective depth to 90 meters with stability class 'A', the predicted concentration matches the measured concentration. The results for all stability classes are shown in table 3. It can be seen that the effective depths listed in table three correlate with the point at which the box model predicted flux line crosses the stability class specific flux in figure 6. This shows that for source depths that are less than the effective depth, the box model is indeed a conservative estimate of flux. It is important to note that as the source depth used in the box model decreases the predicted concentration by ISC-STv3 will increase and as the depth increases the predicted concentration will decrease. For source depths that are smaller than the effective field depth outlined in table 3, the actual source depth should be used. This will lead to large estimations of the flux from sources that have significantly less upwind distance than the effective depth. The over prediction for smaller sources is due to the overestimation of plume height by the box model.

Table 3. Effective depth and resulting flux required for the box model and ISC-STv3 to predict 200µg/m^3 downwind of the source.

	Stability Class					
	A	B	C	D	E	F
Effective Depth (m)	90	126	192	324	453	780
Emission Flux (µg/m^2/s)	35.6	25.4	16.7	9.9	7.1	4.1

Table 3 shows that as the atmosphere becomes more stable, the effective depth of the field increases dramatically. This is driven in ISC-STv3 by the σ_z stability parameter. For more stable atmospheres the vertical plume spread decreases and more of the plume is represented by the 4 meter high box. Due to the large range of effective depth, it is necessary to determine which effective depth, or combination thereof, to use when determining an emission factor.

The stability class and resulting effective depth is a function of wind speed, solar radiation, and cloud cover. In order to find a representative effective depth it was necessary to determine a representative distribution of stability classes for the region in which the box model was to be used. The facility of interest is located in central Texas. Therefore, five years of meteorological data was obtained from the Texas Commission on Environmental Quality's (TCEQ) website (2003). This is the data presented for use in dispersion modeling for permit applications for this area. The first year of the data was used to determine a stability class distribution, and the following four years was used as verification data. Since the stability class is highly dependant on solar radiation, it was decided to divide the data into two groups delineated at 6am representing daytime,

and 6pm representing nighttime conditions. This is an appropriate delineation due to the absence of a significant number of stability classes other than ‘D’ ‘E’ and ‘F’ in the night time data which are the only stability classes possible during this time. Figures 7 and 8 show the day and night time relative frequency distribution of stability classes for the data recorded in Stephenville, Texas in 1985. The relative frequency data was then used to determine a weighted average of the effective field depth from table 3.

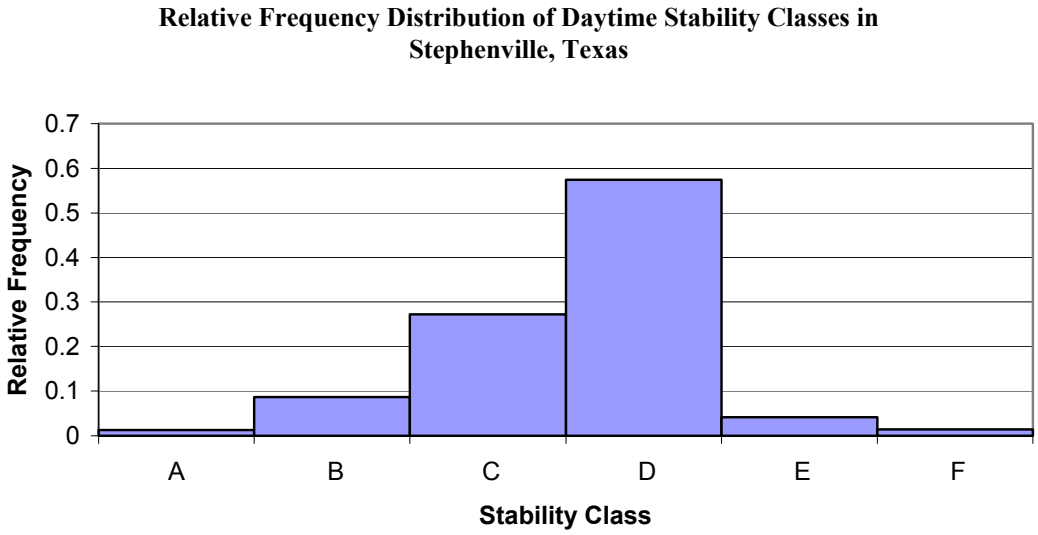

Figure 7. Relative frequency distribution of stability classes for the hours of 6am to 6pm in Stephenville, Texas in 1985.

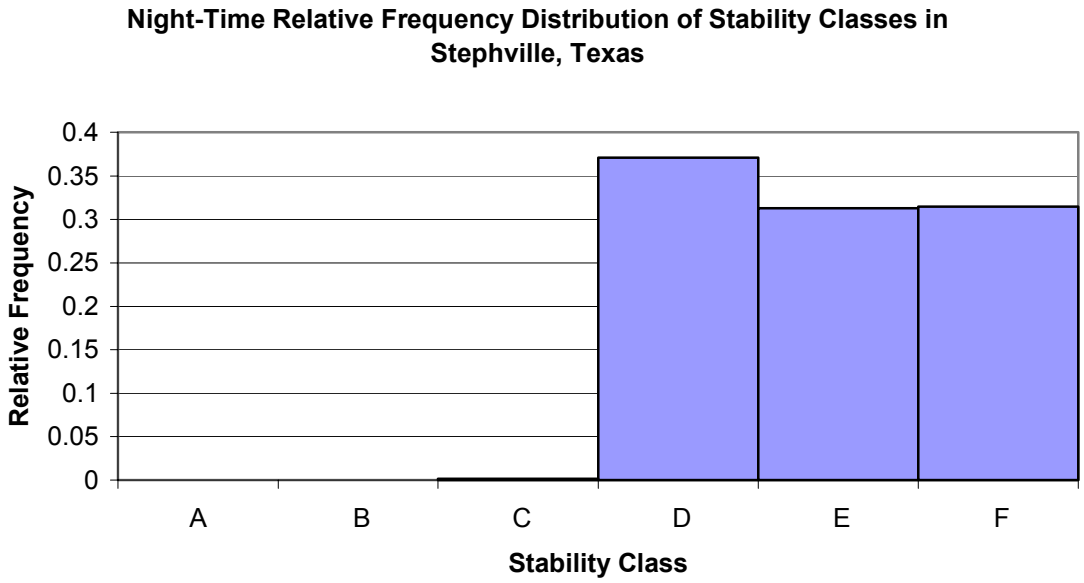

Figure 8. Relative frequency distribution of stability classes for the hours of 6pm to 6am in Stephenville, Texas in 1985.

The resulting effective depth for the day time is approximately 250 meters and approximately 500 meters for night time.

Table 4 shows the results of using the stability class distribution for a year in Stephenville Texas, and the effective source depth developed above. While some stability classes provide an underestimation of the flux resulting in a corresponding underestimation of the measured concentration ($200\mu g/m^3$), the average predicted flux for the entire year is conservative. This is based on the average predicted concentration being greater than $200\mu g/m^3$ for both day time and night time periods.

Table 4. The ISC-STv3 predicted concentration for a daytime field depth of 250 meters and night time field depth of 500 meters using an ideal wind direction. The average concentration was determined by using the relative frequency distribution of stability classes from Stephenville, Texas.

Stability Class	A	B	C	D	E	F	Average
Day Time Predicted Concentration (μg/m3)	91	118	163	344	307	452	272
Night Time Predicted Concentration (μg/m3)	50	68	95	146	188	280	201

The average concentration for both the day time and night time predictions yields conservative estimates for this distribution of stability classes. To effectively use this method a significant number of samples must be obtained that are representative of the sampling population used in this research. Otherwise, the stability class specific effective depth should be used for each sampling period in order to provide more consistently conservative estimates.

Cosine(θ) Effect on Emission Flux Prediction

Using the effective source depth method explained above, it is possible to always determine a conservative estimate of the flux for ideal wind directions. During sampling, it is not likely to have ideal wind directions at all times. Therefore, the algorithm used to determine the effect of wind direction in the box model is critical to determining an accurate emission flux. The model that is currently used applies a cosine(θ) term to the wind speed variable in order to attempt to account for the change in

wind direction. There is no explicit explanation of the reasoning for this addition in the literature, but it appears to be added as an attempt to account for the component of the wind vector that is perpendicular to the downwind edge of the box, thus representing the pollutant that would travel through the downwind plane. This is similar to the method suggested by Turner (1994) for accounting for variations in wind direction when modeling infinite length line sources. This adjustment of the ideal model to account for wind direction yields trends in the flux prediction that are opposite of that which is predicted by ISC-STv3.

To make comparisons between ISC-STv3 and the box model easier, equation 8 is rearranged to form equation 15, which predicts a flux given the other information. Equation 15 can now be used for direct comparisons of predicted concentrations with ISC-STv3 using the same input parameters of wind direction, source dimension, and stability class. By rearranging the equation in this manner, a conservative estimate is now represented as a lower concentration versus ISC-STv3. This is due to the need to increase flux in the box model to match a higher ISC-STv3 predicted concentration.

$$C = \frac{Q_A \bullet X \bullet W_S}{U \cos(\theta) \bullet H \bullet W_B} \tag{15}$$

Figure 9 shows the general trend of predicted concentration versus wind angle for the box model. For ISC-STv3, it is significantly more difficult to generalize the trend of concentration versus wind direction. This is due to the complicated interaction between

the source depth and the vertical dispersion parameters, in connection with the atmospheric stability class.

First, it is desired to determine the trends of each of the algorithms in predicting concentration versus wind direction. In order to compare the concentration predictions across a large number of variations in source configuration and stability class, the concentrations were normalized to the ideal wind direction concentration. This was done by dividing the set of concentrations predictions by the ideal wind direction prediction. This allows for easier analysis of these trends. The earlier effective depth analysis showed the ability to force the box model into a conservative estimate for ideal wind directions, therefore, when analyzing the variation in wind direction it is only necessary to ensure that the box model (or modification thereof) predicts a lower concentration as wind direction deviates. This is represented here by a lower concentration ratio than the ISC-STv3 trend lines.

ISC-STv3 predicts a diminishing concentration trend as the wind direction deviates from ideal for large square sources as seen in Figure 9. As the source depth decreases, ISC-STv3 predicts that the wind angle will have a smaller effect on the concentration, eventually leading to a small increase in the predicted concentration as the wind varies to 45 degrees from ideal. Conversely, the box model predicts an increasing trend as the wind direction deviates from ideal regardless of source dimensions. The trends in figure

9 represent a significant problem with the box model because the prediction of a higher concentration indicates that the box model is not conservative.

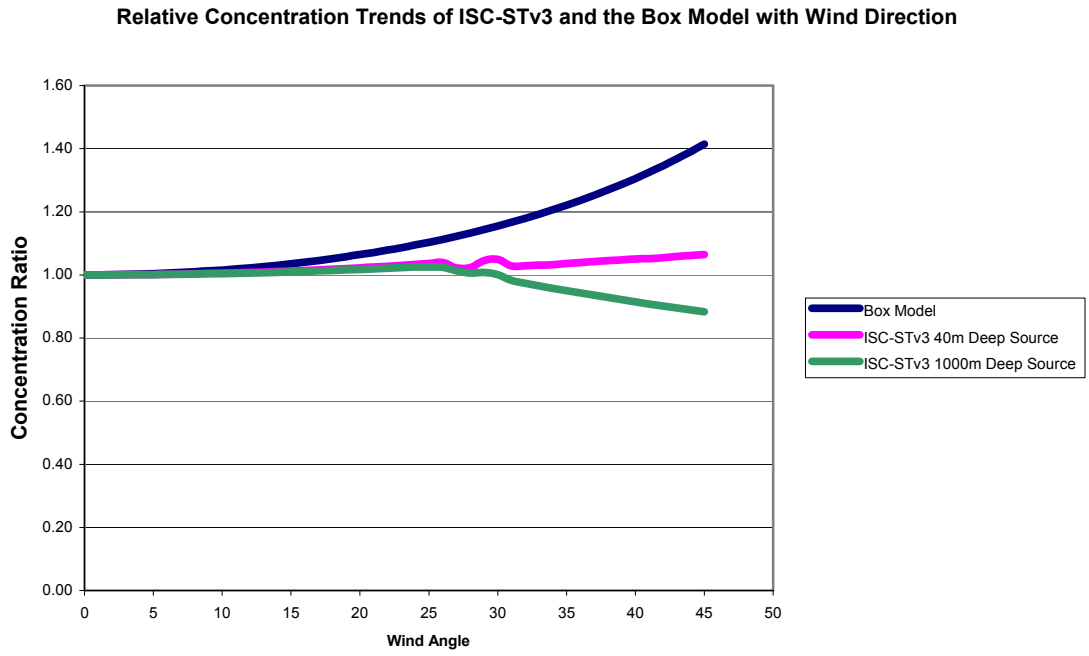

Figure 9. Relationship between concentration and wind angle for both the box model and ISC-STv3. The sources considered are a 40 meters deep and 1000 meters deep. Stability class 6 was used because it represents broadest differential in ratios between the two source types.

The trend in the box model plot in figure 9 is due to the cosine (θ) component. The assumed rationale for using the cosine (θ) component is to account for the perpendicular component of the pollutant transport through the downwind edge of the box. The actual effect of this method can be seen by closely examining equation 15. By looking at the units represented in equation 15 it can be seen that the numerator of the equation represents the total mass emission rate of pollutant, while the denominator represents the volumetric flow rate of the air that travels through the box. By inserting the cosine (θ) term it reduces the total volume of air in which the pollutant is dispersed. This process

increases the predicted concentration in a sinusoidal manner to approximately 1.4 times the ideal wind direction measurement, compared to the decrease of as much as 20% using ISC-STv3. This represents a significant underestimation of the flux by the box model when comparing it to ISC-STv3. This would be unacceptable to the regulatory agencies because their primary mission is to protect the public. Therefore, the question remains as to how to adjust the box model so as to provide consistently conservative estimates of flux.

Wind Speed Model

The simplest method that may be used to ensure a conservative estimate from the box model is to remove the cosine component from the box model equation. This action would make the box model predict the same concentration for a given source receptor configuration, regardless of wind speed. While simple, this model falls short of explaining any part of the trend in ISC-STv3.

Figure 10 shows the relationship between ISC-STv3, the box model, and the wind speed model. Figure 10 shows that the wind speed model is conservative for the 40 meter deep source but is not conservative for the 1000 meter deep source. Due to the downward trend of the concentration versus wind angle in ISC-STv3, there is only one way to ensure a conservative prediction with this approach. This would be to assume a worst case scenario and recalculate the effective source depth for the extreme scenario of maximum wind deviation. This is not realistic because it is assumed that receptors will

be oriented to make the ideal wind direction the most common, according to source configuration and local meteorological conditions. Therefore, by forcing the model to be conservative in the extreme scenario it would drastically over predict the emissions from the source and represent unfair regulation to the source of interest.

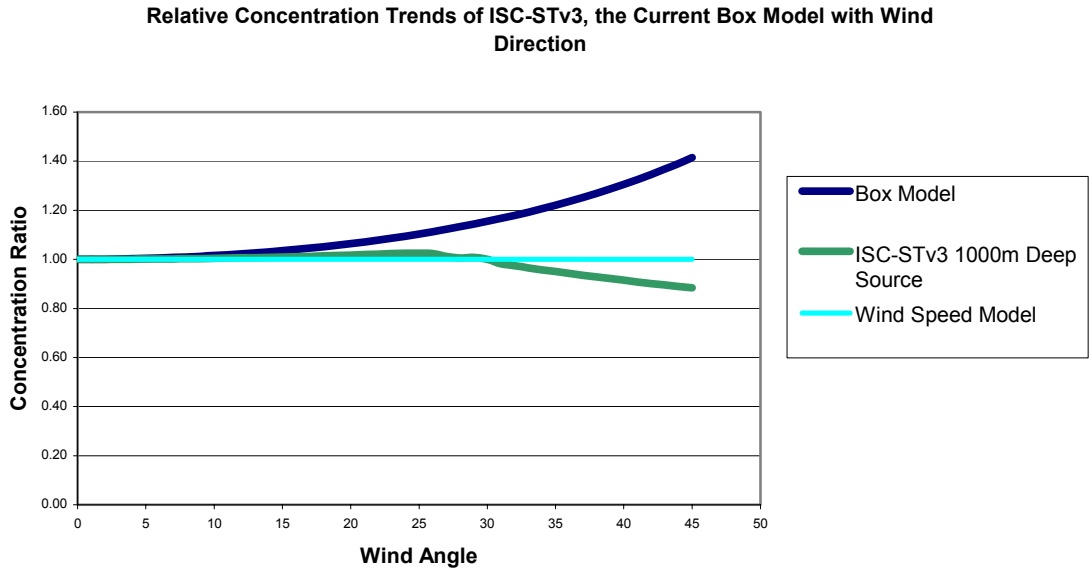

Figure 10. Relative concentration change with varying wind direction with varying wind direction using ISC-STv3, the box model and the wind speed model.

Total Air Flow Model

The next method, the total air flow (TAF) model, attempts to account for the total air flow through the box by calculating the airflow through both the downwind edge of the box, as well as the crosswind edge of the box. The addition of the air flow through the crosswind edge of the box is done by adding the sine term to the denominator of equation 15 to create equation 16. The result of this change is that, for large field depths,

concentration predictions from the box model follow the trend seen in figure 9. The actual predicted concentration in this case is not as important as the trend of the prediction.

$$C = \frac{Q_A \bullet X \bullet W}{\left(U \cos(\theta) \bullet H \bullet W\right) + \left(U \sin(\theta) \bullet H \bullet X\right)} \quad (16)$$

where:

- Q_A = emission flux ($\mu g/m^2/s$);
- X = field depth (m);
- U = wind speed (m/s);
- θ = deviation of wind direction from ideal;
- H = box height (m);
- W = downwind box width (m); and
- X = effective box depth (m).

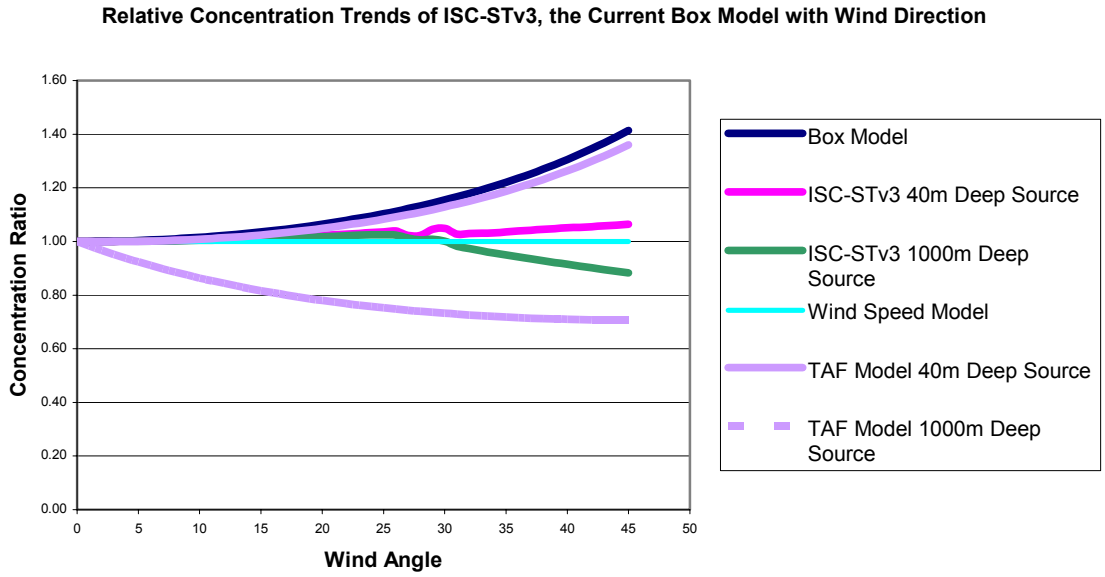

Figure 11. Relative concentration change with varying wind direction using ISC-STv3, the box model, the wind speed model, and the total air flow method.

Once again the TAF model does not yield consistent results for varying combinations of source width and depth. As source depth begins to decrease and becomes significantly less than the maximum effective depth for a stability class, the predicted concentration begins to increase drastically as seen in figure 11. This is attributed to the continued decrease in the denominator due to the cosine term, while the sine term does not increase enough to account for it, due to the limited field depth.

The lack of a conservative estimate for sources without significant depth is particularly troubling for application of this model to dairies,, due to the free stall structures that this source represents. This model could be made conservative by basing the effective source depth on the extreme case of a 45 degree wind direction deviation from ideal. By

adjusting the effective depth this way it would cause significant over prediction of the emission factor leading to unfair regulation of the target source. Therefore, this method of modifying the box model is not ideal.

Inverse Cosine(θ) Box Model

The inverse cosine box model (ICBM) method simply inverts the location of the cosine term in the box model equation; however there is no engineering justification for this method. Equation 17 represents a smooth decrease in the concentration as the wind direction deviates from ideal to 45 degrees.

$$C = \frac{Q_A \bullet X \bullet W_S \bullet \cos(\theta)}{U \bullet H \bullet W_B} \tag{17}$$

The final concentration is 0.707 times the maximum concentration predicted at the ideal wind direction. This ratio compares favorably to that seen for two source configurations seen on free stall dairies. ISC-STv3 predicts a large range for the maximum to minimum predicted concentration ratios. Table 5 shows these ratios, and shows that the 0.707 ratio is always conservative compared to those for ISC-STv3.

Table 5. The concentration ratio of ideal wind direction to a 45 degree deviation of wind direction for two typical source configurations found on free stall dairies for both ISC-STv3 and the ICBM.

	Stability Class					
	1	2	3	4	5	6
40 Meter Deep Source	1.01	1.03	1.03	1.05	1.06	1.06
1000 Meter Deep Source	0.92	0.91	0.90	0.89	0.88	0.88
Box Model	0.71	0.71	0.71	0.71	0.71	0.71

This method provides a conservative estimate for the flux compared to ISC-STv3 for all source configurations and stability classes. Figure 12 shows how this method compares to all the others previously discussed. It should be noted that this model is not dependant on source depth to be conservative across the range of desired wind directions. This is valuable because it is now only necessary to ensure that the ideal wind direction estimate is conservative. Once the ideal wind direction is conservative for a given stability class, all estimates of the emission flux will be conservative.

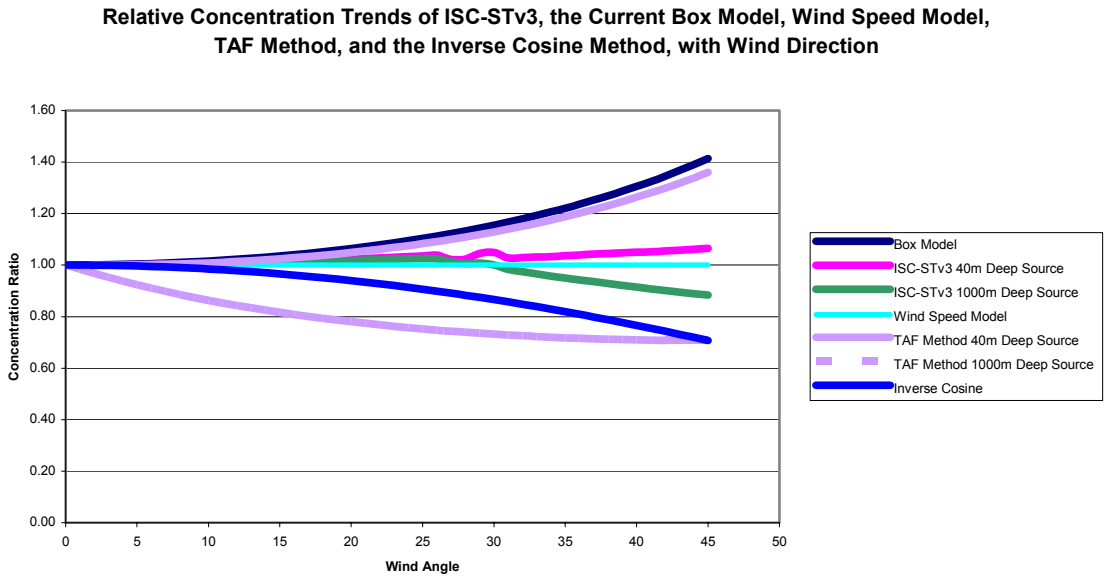

Figure 12. Relative concentration trends of ISC-STv3 and all the different box model modifications. The only consistently conservative model is the ICBM represented by the solid blue line.

Results and Discussion

By combining the effective depth limitations and correcting the cosine(θ) component of the box model, it is possible to generate a conservative estimate of the flux for all sources that are expected to be on a free stall dairy. In order to verify this, two sources are going to be used to test the validity of the model. The first is a long narrow source that is 50 meters deep and 200 meters long, which will represent the free stall structure on a free stall dairy. The second source, is a square source that is 200 meters square, will represent an open pen area on a free stall dairy. The receptor for the model will be placed in the ideal location as presented earlier, at the downwind edge, center of the source.

In order to evaluate the box model it will be used to develop an emission flux from each source, for all wind directions between ideal and 45 degrees deviation, using a theoretical measured concentration of 200 $\mu g/m^3$. The resulting emission flux will be used in ISC-STv3 to predict a concentration using the same wind direction and wind speed for each stability class. As long as the ISC-STv3 predicted concentration is always higher than the beginning concentration of 200$\mu g/m^3$, the box model will be conservative.

Figure 13 shows the predicted concentration for a 200 meter wide by 50 meter deep source using the ICBM to determine the input fluxes. This shows that for all stability classes across the entire range of wind directions the ISC-STv3 prediction of concentration is always higher than the beginning concentration of 200$\mu g/m^3$. This verifies that the modified cosine box model is indeed conservative for this type of source. It is important to note that this process will provide significant over estimation of the flux for more stable stability classes, as seen in figure 13. The over prediction of this method is revealed by the significant over prediction of concentration by ISC-STv3, by as much as 10 times the theoretical measured concentration. This is because the actual source depth is significantly less than the maximum effective depth for a 4 meter box height. The 4 meter box height with a uniform concentration, significantly over represents the plume height at the sampler location. The less stable the atmosphere, the closer the source depth is to the effective depth; meaning that the 4 meter box height more accurately represents the actual plume.

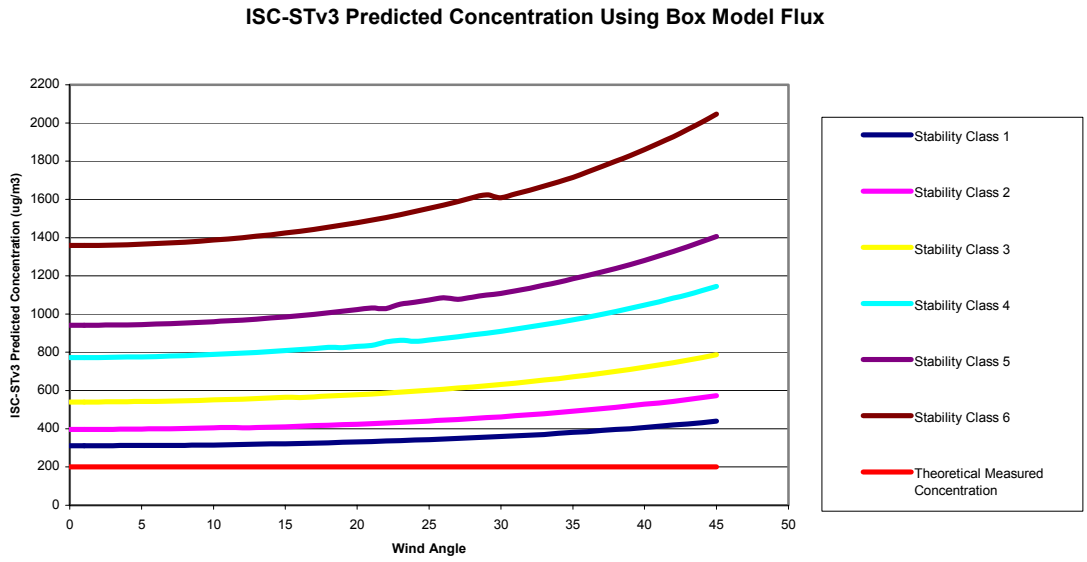

Figure 13. The ISC-STv3 prediction of concentration using the ICBM as a flux input for all stability classes for a source that is 200 meters wide by 50 meters deep.

For sources with larger depths there exists less over prediction of the flux by the box model for the differing stability classes. This is because the source depth is closer to the effective depth of the different stability classes. This can be seen in figure 14, in that there is not the extreme over prediction of the flux for the higher stability classes. The maximum over prediction of the concentration, which is directly proportional to emission flux, is on the order of 3.25 times the actual concentration. The stability classes that have an effective depth that is less than that of the depth of the source, over estimate the concentration by less than 50% at the extreme wind direction. This represents relatively good agreement, while always being conservative.

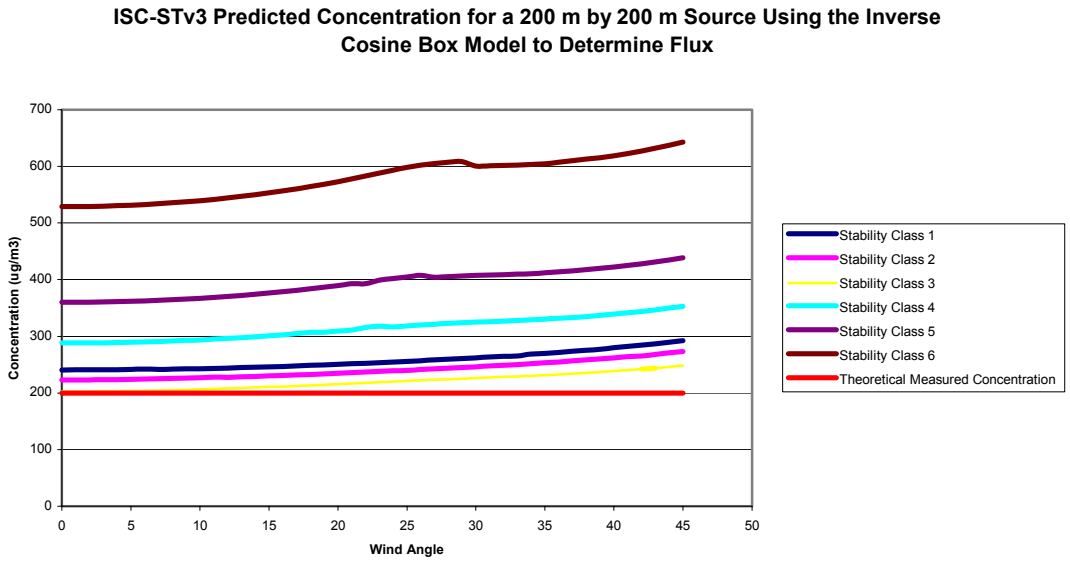

Figure 14. The ISC-STv3 prediction of concentration using the ICBM as a flux input for all stability classes for a source that is 200 meters wide by 200 meters deep.

Conclusions

The fixed height box model initially proposed by Flocchini et al. (2001) does not accurately represent the trends of ISC-STv3 for varying wind directions. By limiting the box height to 4 meters the effective depth that is represented by the model is limited according to the ISC-STv3 analysis. The cosine (θ) component introduces trends in the model that are the opposite of those that are produced by ISC-STv3. This represents a possible source of underestimation of the emission flux when this model is used with extreme variations in the wind direction. By altering the box model equation by inverting the cosine(θ) term, the trend in the box model more accurately reflects the trends found in ISC-STv3.

By developing an effective source depth that corresponds to the 4 meter box height and is dependant on stability class, it is possible to ensure that for ideal wind direction, the box model will always be conservative. By inverting the cosine (θ) term in the box model, it is also possible to ensure that the estimate of flux by the box model remains conservative for deviation of wind direction by as much as 45 degrees from ideal. Both of these adjustments may lead to an overly conservative estimate of the flux.

It must be noted that these conclusions are valid for single sources and ideal conditions. When sources are combined or sampler placement is not ideal, there will be significant variations in the results.

There is a perception by some in the regulatory community that if there is doubt in an emission factor, then it should be higher in order to protect public health. While regulatory action is intended to protect public health, overestimated emission factors do not achieve this goal. Overestimated emission factors will lead to increased regulatory efforts that detrimentally affect the source, due to increased operating costs, while providing no improvements in air quality. Therefore, it is imperative that facility emissions be estimated as accurately as possible using sound science. According to this analysis the variation inherent in any form of the fixed height box model will lead to inaccurate emission factors when compared to ISC-STv3 and therefore, the fixed height box model is a poor tool for emission factor development.

CHAPTER V

EMISSION FACTOR DEVELOPMENT

This chapter intends to use the atmospheric dispersion model known as Industrial Source Complex-Short Term version 3 (ISC-STv3), and the ICBM described in the previous chapter, to estimate the emission from a dairy in central Texas. Ambient TSP sampling was conducted during the summer of 2002 and 2003 at a free stall dairy in central Texas in order to determine ambient concentrations that could be used as inputs into the two models. The emission rate determined through the use of the models and ambient sampling was adjusted downwards to account for seasonal effects such as rainfall. The results of the two models are also compared in order to determine the effectiveness of using the ICBM for emission factor development.

Methodology

Experimental Plan

All sampling was conducted on a central Texas Dairy during the summers of 2002 and 2003. All data arerepresentative of dry summer conditions in Texas. The final sampling period was cut short by significant rainfall. All sampling trips were preceded by hot dry conditions for several weeks.

Facility

Data for this study was collected over multiple trips to a central Texas dairy in the summers of 2002 and 2003. The dairy herd consisted of 1800 milking cattle, with a total of 3,400 head on property. The lactating herd was kept in a series of three free stall structures and two open pens. Each free stall housed approximately 460 cattle, and the two open pens housed approximately 230 cattle each. The layout of the dairy is presented in Figure 15, with the ovals representing sampler locations. The low producing cattle were kept in open pens one and two. These pens had a very similar layout to feed yards in that the pens were paved along the feed lane, with the rest of the area covered by a manure pack. There were small shades in each pen that the animals tended to congregate around during the heat of the day. The remainder of the lactating herd was kept in the free stalls. The free stall structures consisted of paved alley ways for the cattle to walk on, and individual stalls for each animal to lie in. The alley ways were flushed 4 times per day to remove the manure that was deposited in the alley ways by the cattle. The stocking density in the open pen area was approximately 46.5 m^2/head and approximately 9.3 m^2/head in the free stalls.

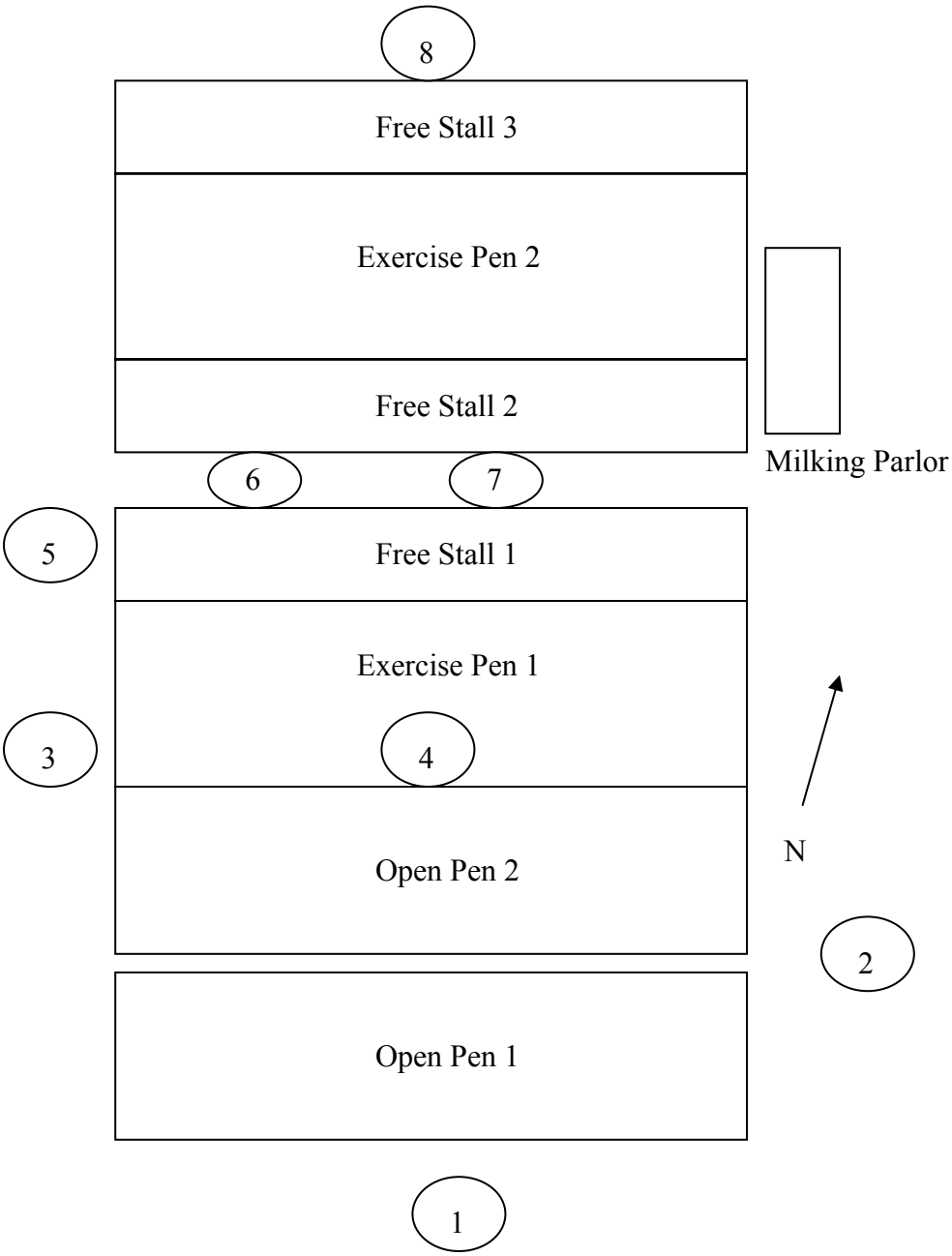

Figure 15. Schematic of the configuration of pens, milking parlor, free stalls, and relative sampler locations. Samplers are indicated with ovals.

Particulate Matter Sampling

Ambient concentrations of particulate matter were determined using a gravimetric approach with multiple types of samplers. The primary type of sampling used was TSP sampling. This was done due to the extensive nature of sampling bias that has been documented by Buser et al. (2001). The primary sampler used for this work was a high volume TSP sampler built according to the TSP reference method (USEPA, 2002). The samplers work by drawing air through a filter element that measures 20.3 cm by 25.4 cm. The net mass collected on the filters is determined and divided by the volume of air sampled to determine the ambient concentration. The design of these samplers was meant to mimic the human respiratory system, with a cut point of approximately 40μm AED (Parnell et al., 1999). The samplers used in this project were designed specifically for the extreme conditions that were expected to be encountered on the dairy. The sampler design is described by Boriack et al. (2003). The air handling was much more durable and the samplers were made to be more mobile as well. The increased durability was achieved through the use of heavy duty centrifugal fans (HP-33, Cadillac Products, Chicago, IL), with an adjustable rheostat to control air flow.

Measuring the Volume of Air Sampled

In order to accurately determine concentration, two variables must be known, total air flow and the total mass of PM sampled. Total air flow was determined through the use of a sharp edge orifice mounted between the filter and the fan housing. The pressure

drop across the orifice was measured using a magnahelic gauge (Cat. No. 2005, Dwyer Instruments, Michigan City, IN) and used to determine instantaneous volumetric air flow.

The Bernoulli equation was used to relate the pressure drop across the orifice meter to air flow rate.

$$Q = 3.478kd^2\sqrt{h/\rho} \tag{18}$$

where:

- Q = flow rate of air through the orifice meter (m^3/s);
- k = empirical constant;
- d = diameter of the orifice (m);
- h = pressure change across the orifice meter (mm H_2O); and
- ρ = density of air (kg/m^3).

The empirical constant was determined experimentally once for each sampler in the lab before field sampling took place. This was done by placing a laminar flow element (LFE) (Model 50MC2, Meriam Instruments, Cleveland, OH) in series with the orifice meter and fan assembly. The LFE allowed for determination of actual flow rates through the fan. The fan was then adjusted across multiple flow rates, and the pressure drop across the orifice was then measured using a hand held manometer with an accuracy of ±0.5% of full scale (Mark III Series 475-FM Dwyer, Michigan City, IN).

Equation 18 was solved for 'k,' and the density of air (ρ) in the lab was calculated using equation 19.

$$\rho_{ma} = \frac{(P_b - \phi P_s)(M.W.)_{da}}{RT} + \frac{\phi P_s (M.W.)_{wv}}{RT} \qquad (19)$$

where:

- P_b = barometric pressure (atm)
- ϕ = relative humidity (fraction);
- P_s = saturated water vapor pressure (atm);
- MW_{da} = molecular weight of dry air (gmol);
- MW_{wv} = molecular weight of water vapor (gmol);
- R = universal gas constant (atm-l/gmol-K); and
- T = air temperature (K).

In order to calculate the saturated water vapor pressure, equation 20 was used (ASAE Standards, 1999).

$$\ln\left(\frac{P_s}{R}\right) = \frac{A + BT + CT^2 + DT^3 + ET^4}{FT - GT^2} \qquad (20)$$

where:

- T = Temperature (K);
- R = ideal gas law constant; and
- A through G are empirical constants.

Once the orifice constant ‘k’ was determined for each sampler, the precise flow rate could be determined by measuring the pressure drop across the orifice meter during sampling. This was done using a pressure transducer (Omega PX274, Omega, Stamford, CT). The accuracy of the pressure transducer was reported as ± 1% of full scale by the manufacturer. The 4-20 ma output from the pressure transducer was recorded every 12 seconds with a data logger (HOBO H8 RH/Temp/2x External, Onset Computer Corporation, Pocasset, MA). The air density for each test was calculated using actual meteorological conditions recorded during the test by the meteorological station on site. Average air density was calculated during each sampling period and assumed to be constant during each test. An instantaneous air flow was determined each 12 seconds during the test, which was assumed to be constant and therefore, could be summed to determine total air flow for each test.

The previously mentioned pressure transducers were also calibrated prior to each sampling trip. This was accomplished by generating a constant pressure that was fed into the high side of both the pressure transducer and the hand held manometer. The output of the pressure transducer was measured using a multimeter and plotted against the measured pressure. Linear regression was then used to relate the output amperage to the measured pressure.

During sampling a HOBO weather station (H21-001, Onset computer Corporation, Pocasset, MA) was used for all meteorological data collection. The station used a

temperature/RH sensor (S-THA-M002, Onset computer Corporation, Pocasset, MA) with a reported accuracy of ±0.7°C at 25°C and ±3% RH. The solar radiation was measured using a silicon pyranometer (S-LIB-M003, Onset computer Corporation, Pocasset, MA) with a reported accuracy of ±10 W/m^2. The wind speed and direction were measured on 5-minute intervals using a wind speed/direction sensor (S-WCA-M003, Onset computer Corporation, Pocasset, MA) with a reported accuracy of ±0.5 m/s and ±5°. Finally barometric pressure was measured with a barometric pressure sensor (S-BPA-CM10, Onset computer Corporation, Pocasset, MA) with a reported accuracy of ±1.5mbar. All measurements were recorded on 5-minute averages for the duration of each sampling trip, except the barometric pressure which was only recorded hourly.

It was assumed that the temperature, RH, and barometric pressure varied minimally between recording intervals. The mean temperature, barometric pressure, and relative humidity were used during each sampling period to calculate the average ambient density for that sampling period.

Measuring the Mass of Particulate Matter Collected

Two types of filters were used during sampling for various reasons. The primary filter media used was glass fiber filter paper. The second type of media used was a Polyetrafluoroethylene (PTFE) filter for particle size analysis. Both filters were weighed three times both prior to and after sampling in order to determine the mass collected on

the filter. The weighing was conducted using a high precision balance (AG245, Metler Toledo, Greifensee, Switzerland), in a controlled environment room (temperature ≈25°C, relative humidity ≈50%). The conditions were required to be identical for both the pre-weighing and post-weighing of the filter, in order to minimize the effects of relative humidity. Therefore, the filters were always conditioned for at least 24 hours in the weighing environment prior to actual weighing. During the actual weighing process each filter was weighed three times, and the average of the measurements was used.

During field sampling the filters were held to the samplers using standard filter holder cartridges (Graseby Andersen/GMW, Smyrna, GA). The filters were placed in the cartridges in a mobile sampling laboratory. All filter handling was done with latex gloves in order to minimize contamination of the filter media. The filter cartridges were then covered and transported to each field sampler in an airtight container. The filter cartridge was placed on the sampler and the cover removed immediately prior to sampling. Due to the continuous nature of sampling, the previous cartridge was removed, covered and placed in a separate container for transport back to the mobile sampling lab. Upon returning to the mobile sampling lab, the filters were carefully inspected for holes or tares and removed from the cartridge to be replaced by a new filter for the next sampling period. During each day, multiple filters were transported to and from the sampling locations, but not used to monitor for any contamination.

Sampling Procedure

Sampling was conducted during one week periods in the summer. The 2002 sampling excursion consisted of sampling primarily between the hours of 8 am and 8 pm for 4 days. The summer 2003 sampling excursion consisted of sampling 24 hours per day for approximately 4 days. Samplers were placed such that they were as close to the middle of the plume from the target source as possible. However, this was not always viable due to the configuration of the facility. Each sampler location consisted of the sampler and a generator that was used for power. The generator was always located downwind of the sampler, at least 5 meters away, in order to minimize its effect on the ambient concentration.

Individual sample duration varied between 2 and 4 hours, depending on the ambient conditions. This sample duration was selected in the hope that there would be a measurable amount of mass on the filters, while at the same time minimizing wind direction variation during the individual sampling period.

Particle Size Analysis

TSP sampling represents the total amount of suspended particulate in the ambient air. The regulated pollutant of interest is a subset of TSP called PM_{10}. In order to relate PM_{10} to TSP it is necessary to determine the particle size distribution (PSD) of the collected mass. This would allow for a direct measurement of the amount of total mass

collected that is less than 10 micrometers. Particle size analyses were performed using the Coulter Counter Multisizer (CCM) (Beckman-Coulter, Coulter Multisizer III, Miami, FL). The CCM works on the basis of the Coulter electric sensing zone principle to determine particle count and individual particle volume. In order to achieve this, the particles are suspended in an electrolyte solution of 5% lithium chloride in ethanol. The solution of suspended particles is then passed through a small orifice, with electrodes on both sides, through which a current is passed. As the particle passes through the orifice it displaces a volume of electrolyte equal to its own volume. The displacement of electrolyte increases the impedance across the orifice in an amount proportional to the volume of the particle. This process results in an output of particle volume versus equivalent spherical diameter (ESD).

Aerodynamic equivalent diameter (AED) is the basis for regulation of particulate matter. Therefore, the ESD must be converted to AED through equation 21 (Cooper and Alley, 2002).

$$D_a^2\left[1+\frac{\lambda}{D_a}\left(2.514+0.8e^{\left(-0.55\frac{Da}{\lambda}\right)}\right)\right]=\frac{\rho_p D_p}{\rho_w}\left[1+\frac{\lambda}{D_p}\left(2.514+0.8e^{\left(-0.55\frac{Da}{\lambda}\right)}\right)\right] \quad (21)$$

where:

- D_a = aerodynamic equivalent diameter;
- λ = mean free path of air, 0.066 meters;
- D_p = equivalent spherical diameter;
- ρ_p = particle density; and

- ρ_w = density of water.

This equation simplifies to the following equation (Cooper and Alley, 2002).

$$D_a = D_p \sqrt{\rho_p} \tag{22}$$

In order to conduct the CCM particle size analysis, a portion of the filter is cut from the entire filter and placed in the lithium chloride ethanol solution. The particles are separated from the filter using a sonic bath. Due to the nature of the glass fiber filters, they are unable to be used for this analysis, except when extremely high concentrations are measured. Therefore, this was conducted on the PTFE filters only since they do not produce any particles when cut apart. Once the particles are suspended in the solution the CCM analysis is conducted by counting approximately 300,000 particles in the solution.

The resulting particle size distribution is fit to a lognormal curve defined by the MMD and the geometric standard deviation (GSD). The GSD is defined as the ratio of the MMD, or d_{50}, to $d_{15.9}$ or the ratio of $d_{84.1}$ to d_{50}. The PSD was used to determine the mass of PM_{10} of the sampled TSP in order to calculate PM_{10} emission rates.

Sampling Scheme

The sampling scheme varied throughout the experiment in an attempt to obtain the most representative data during each sampling excursion. Therefore, all locations labeled on

Figure 15 were never operational at the same time. The sampling array was designed to take advantage of the prevailing southerly winds by placing samplers on the northern edge of the identified emissions sources, the free stalls and the open pen area. The locations were chosen in an attempt to have each sampler located in the plume from one source or the other, as much as possible, while at the same time avoiding interference with the daily operations of the dairy. The resulting sampling array is shown in Figure 15.

During the period of sampling at the dairy, the cattle in the free stalls were not allowed in the exercise pens. This simplified the sampling scheme by not requiring the separate quantification of emissions from those sources. It is assumed that the emissions from those areas are zero for modeling purposes.

Emission Rates

Emission rates were calculated using ISC-STv3 and the ICBM method. ISC-STv3 is an EPA preferred model for predicting concentrations from area sources for regulatory purposes, and was chosen because it may be used to determine compliance with future regulatory action of these facilities. The ICBM model is used in Chapter III to evaluate its effectiveness with more complex facilities.

ISC-STv3 is typically used to predict concentrations given emission fluxes, and must be used in reverse for the determination of emission fluxes from measured concentrations.

As explained earlier, it is not possible to directly solve Equation 9 for an emission flux given a concentration, therefore a multi step process must be used. This process involves entering the facility dimensions, receptor locations, and the pertinent meteorological data into ISC-STv3 with an emission flux of 1μg/m^2-s. Upon executing the model, a unit flux concentration (UFC) is predicted at each receptor location. The UFC represents the predicted concentration at the receptor per 1μg/m^2-s emission flux. Using this principle Equation 23 can be used to determine emission flux.

$$EF = \frac{C_{measured}}{UFC} \tag{23}$$

where:

- EF = emission flux (μg/m^2-s);
- $C_{measured}$ = measured concentration (μg/m^3); and
- UFC = unit flux concentration (μg/m^3/(μg/m^2-s)).

ISC-STv3 was used to determine the UFC for each sampling period. The model was used with regulatory default options. All sampler heights were 1 meter as they were in the field. Meteorological data was used on 5 minute averages for the duration of each test. For example, a 2-hour test would consist of 24, 5 minute meteorological input values. This allowed for more accurate representation of actual transport by accounting for more wind variation during the sampling period. The 5 minute meteorological inputs also more accurately reflect the conditions used to develop the dispersion parameters.

Upon determining the emission flux for a given sample, from a specific emission source, it must be converted into a mass per animal per time. This is done by multiplying the emission flux by the animal spacing per 1,000 head, and converting to a daily basis. For the free stall area the animal spacing was 8700 m^2/1000head of animals. For the open pen the animal spacing was 42,600 m^2/1000head

For most sampler locations there was only one source contributing to the concentration as determined by ISC-STv3. For receptor locations 5, 6, and 7 many sampling periods had emissions from both the open pen and the free stalls contributing to the concentration. In order to develop a valid emission flux for these locations it was imperative to have a known emission flux from one of the sources. This was determined by using the nearest sampler that was affected by only one source. Therefore, the open pen emission rate, as determined by sampler 3 was used to determine the open pen contribution to that measured concentration. This value was then subtracted from the net measured concentration to determine a new net measured concentration that could be used to scale the free stall emission flux. Due to the sampling configuration receptor location 3 typically only had contributions from the open pen area and was used to determine the emission flux from this area with no confounding sources.

The ICBM method as described in the previous chapter, is different only in that once a total mass emission rate is determined through the downwind edge of the box, it is divided by the total number of head upwind of the sampler to determine a mass per head

per day. The assumption used in this method is that all emissions upwind of the sampler are uniform. Therefore, there is no method for differentiating between sources upwind of the sampler location. This is a significant limitation of ICBM in this situation.

Seasonal Variation

Emission rates calculated directly from sampling data do not accurately characterize the emissions on a full year basis, due to the conditions present during sampling. Emission rates developed from sampling during dry summer conditions only characterize the emissions during those same dry summer conditions. Therefore, it is necessary to adjust the emission rate to account for variations in emissions that will occur throughout the year. This can be done by accounting for rainfall events that will suppress emissions. Due to the meteorological conditions present while sampling, the emission rate developed directly from those sampling events represents a maximum emission rate during the year, for most areas of the country.

To account for the affects of rainfall on PM emissions from a dairy, it is necessary to determine the amount of rainfall necessary to suppress PM emissions. Parnell et al. (1999) assumed that any effective rainfall event greater than ½ the local reference evapotranspiration (ET) will suppress dust emissions. Further they assumed that the duration of emission suppression was proportional to the difference between effective rainfall and ET. That is to say that if the effective rainfall for an event was twice the daily ET rate, then the length of suppression would be 2 days.

The USDA-NRCS curve number equations are used to determine the difference between runoff volume and precipitation volume, referred to as effective rainfall. The effective rainfall is then used to determine the amount of ET that must occur before emissions continue. Equations 24 through 27 (Haan et al., 1994) show the process used to determine effective rainfall.

$$S = \frac{25400}{CN} - 254 \tag{24}$$

$$Q = \frac{(P - 0.2S)^2}{P + 0.8S} \; for(P > 0.2S) \tag{25}$$

$$Q = 0 \; for(P < 0.2S) \tag{26}$$

$$ER = P - Q \tag{27}$$

where:

- S = maximum soil water retention parameter (mm);
- CN = USDA curve number (90);
- Q = runoff volume (mm);
- P = precipitation volume(mm); and
- ER = effective rainfall (mm);

The curve number was selected to represent a soil type with high runoff and little infiltration. The amount of rainfall that must fall before runoff occurs is represented by the 0.2S parameter with a threshold of 5.64mm.

The next step is to determine the duration of dust suppression provided by a rainfall event. It is assumed that as long as the sum of the effective rainfall exceeds the sum of the ET since that rainfall, there is sufficient soil moisture to suppress dust emissions. In order to accurately characterize the ET and the rainfall for a given region, extensive historical records of ET and precipitation are required. This data is easily available for some regions like California's San Joaquin Valley. This is an ideal region to use due to its high density of dairies, combined with the poor air quality.

In order to quantify the suppression of emissions due to rainfall events, it is necessary to determine the frequency of rainfall events of varying intensity, as well as the duration required to remove the moisture in the manure pack. Therefore, it is necessary to determine the quantity of rainfall that will suppress emissions for a given amount of time. Parnell et al. (1999) used three classes to characterize the dust suppression of effective rainfall.

- Class 1 is assumed to be effective rainfall events that total less than the daily ET and will evaporate in a single day. These events span all rainfall less than the local ET. Therefore, they are represented by the probability of a rainfall event being greater than ½ the local ET and were assumed to suppress emission for half a day.
- Class 2 events were those with effective rainfall depths that span from the local Et value to twice the local ET value and are represented by the probability of an

effective rainfall event exceeding 1.5 times the local ET. These events were assumed to suppress emissions for 1.5 days.

- Class 3 events are those with an effective rainfall greater than twice the local ET. These events are associated with the probability of the effective rainfall exceeding 3 times the local ET. These events were assumed to suppress dust emissions for 2 days.

Using these classes to characterize the data acquired from the California Irrigation Management Information System (CIMIS) data center, it is possible to determine the probability of each event occurring in a given month. Table 6 shows the average monthly ET as determined by a 21 year average in California's San Joaquin Valley collected from CIMIS.

Table 6. Monthly ET and effective rainfall amounts associated with each class for California's San Joaquin Valley. Determined from a 21 year average.

	ET (mm)	Class 1	Class 2	Class 3
Jan	0.84	0.42	1.26	2.53
Feb	1.66	0.83	2.49	4.97
Mar	2.87	1.44	4.31	8.61
Apr	4.41	2.20	6.61	13.22
May	5.74	2.87	8.61	17.23
Jun	6.61	3.30	9.91	19.82
Jul	6.42	3.21	9.63	19.26
Aug	5.72	2.86	8.58	17.15
Sep	4.31	2.15	6.46	12.92
Oct	2.76	1.38	4.14	8.28
Nov	1.37	0.69	2.06	4.12
Dec	0.80	0.40	1.20	2.40

Table 7 shows the probability of each class occurring during each month, as well as the probable number of days each month with zero emissions. This is obtained by determining the probable number of days each month in a given class, then weighting that class by the duration of emissions suppression associated with that class, and finally summing across all three classes each month. The total number of emission free days is then the sum of the emission free days each month. The total for the San Joaquin Valley is 88.5 emission free days per year or a 24% reduction in peak emissions.

Table 7. Monthly probability of each class occurring and the associated number of emission free days for California's San Joaquin Valley.

Month	Class 1 Probability	Class 2 Probability	Class 3 Probability	# of Days/mo	Zero Emission Days
Jan	0.25	0.17	0.14	31	20.48
Feb	0.24	0.13	0.12	28	15.38
Mar	0.16	0.10	0.06	31	11.13
Apr	0.07	0.03	0.01	30	3.45
May	0.04	0.01	0.00	31	1.21
Jun	0.02	0.00	0.00	30	0.45
Jul	0.00	0.00	0.00	31	0.07
Aug	0.01	0.00	0.00	31	0.19
Sep	0.05	0.03	0.01	30	2.78
Oct	0.06	0.04	0.02	31	3.50
Nov	0.18	0.10	0.08	30	11.82
Dec	0.23	0.15	0.12	31	18.03
Total Zero Emission Days					88.51

A total of 88.5 emission free days is a conservative estimate of the number of days in a given year that will have emission suppression due to precipitation. There is very little ET during the winter months and many times ET approaches zero due to severe fog events. Therefore, the assumption that a rainfall event will not suppress emissions for more than 2 days is a drastic underestimate of suppression during these months. It is also a conservative estimate due to the assumption that ET rate is representative of the drying rate of the open pen areas. This is not valid due to the fact that it is only soil and therefore, has no transpiration; therefore ET is a high estimate of the drying rate.

It should also be noted that this is a similar number of emission suppressed days as that developed by Parnell, et al. (1999) for the Amarillo, Texas region. Parnell et al., also conclude that a 21% reduction in emissions due to rainfall events is a valid number for

the entire state, for feed yard emissions. This is a logical assumption for dairies as well, due to the extensive number of dairies relocating to the Amarillo, Texas region.

Results and Discussion

Meteorological Data

The meteorological conditions during the two seasons were significantly different. During the 2002 sampling campaign, meteorological conditions were not typical for the region during the sampling event. The prevailing south-easterly winds trended much farther east than usual and were more variable as well. This presented significant challenges for designing a sampling scheme that would work with as much variation as possible. This is the reason that there are several sampling periods that did not yield any results from this excursion. Samplers were initially placed with the expectation of the south-easterly wind. After several sampling periods of wind that was not appropriate, some samplers were moved in order to locate them within the plume that was resulting from the non-traditional winds. There were even some sampling periods, that placed the samplers that were planned as upwind samplers, in the downwind position. In this case they were used as downwind samplers.

The following year resulted in much more traditional meteorological conditions with a prevailing south-easterly wind that was relatively consistent. This resulted in much better sampling recovery. The combination of enough personnel for 24-hour sampling, improved experience with the equipment, and consistent meteorological conditions

resulted in a significantly greater number of samples collected. Although this sampling period was cut short due to approximately 80mm of rainfall on the last two days of sampling, the number of successfully recovered samples is significantly larger than the previous year.

Concentration Measurements

Concentration measurements that are summarized here represent the successfully analyzed samples. There were many samples that were not fully analyzed due to various problems encountered in the field and in the laboratory. Problems with the equipment often lead to very short sampling periods (less than 20-minutes) on some tests. These problems had a wide variety of causes such as fan failure, generator failure and, animal damage. Other samples were abandoned for causes such as torn filters during the handling and transport process. These concentrations were not calculated due to the unknown variable of mass collected on the filter. There were even some experiences of exceptionally poor sampler placement, such as the first 6 tests of the first year, which represented a sampler being placed downwind of a powdered mineral supplement. The cattle would toss the powder in the air while eating and the resulting plume would travel directly toward the sampling location. Once this was observed the sampler was moved.

Measurements recorded during the summer of 2002 had an average upwind TSP concentration of 115$\mu g/m^3$, with a maximum of 231$\mu g/m^3$ and a minimum of 41.4$\mu g/m^3$. The net downwind concentrations averaged, 134 $\mu g/m^3$ with a maximum of 491$\mu g/m^3$

and a minimum of 14μg/m^3. There were a few samples that had a negative net downwind concentration. This correlated to the times the wind direction did not flow across the source to the sampler.

The following season the average upwind TSP concentration was 76 μg/m^3, with a maximum measured concentration of 154μg/m^3 and a minimum of 37μg/m^3. The net downwind concentrations averaged 118μg/m^3, with a maximum of 392μg/m^3 and a minimum of 30μg/m^3.

Particle Size Analysis

Particle size distribution analysis was done only on the PTFE filters that were exposed in the field. This is due to the low background of these filters compared to the high background counts associated with the use of glass fiber filters during the analytical process. A total of 21 samples were analyzed from samplers that were confirmed to be in a downwind location. Another 4 filters were analyzed from sampler locations that were confirmed to be in upwind locations. The mean downwind MMD was 12.9 μm corrected to AED with a GSD of 2.23. The mean upwind MMD was 10.1μm corrected to AED with a GSD of 2.16. The means upwind concentration from these samples was 100μg/m3 and the mean downwind concentration was 230μg/m^3.

This represents a significantly smaller MMD than that reported by Sweeten et al. (1988, 1998) for feed yards. The apparent reason for this difference is the significantly lower net concentrations measured on the filters. The downwind sampler is a composite sample of all the PM in the air and does not only represent the source emissions. This is the reason that an upwind concentration is subtracted from the downwind measured concentration to yield a net measured concentration when calculating emission rates. When determining PSD it is important to use this same process to determine the net PSD or the PSD that is emitted.

It is possible to account for the effect of the upwind PSD on the downwind filters by assuming the downwind sampler represents a combination of the upwind PSD and source PSD, and that they are represented proportionally in the downwind PSD by their mass. For example, using the average MMD and GSD recorded during this test, the upwind sampler measures a concentration of 100μg/m^3 and the downwind sampler measures 230μg/m^3. The upwind PSD has an MMD of 10.1μm and a GSD of 2.16, while the downwind PSD has an MMD of 12.9μm and a GSD of 2.23. In this case the downwind PSD has significant mass associated with it that is not from the source, but from the ambient concentration. This leads to a smaller measured MMD than the actual source emissions. In order to determine the net effect of the source PSD on the downwind sampler, it is necessary to separate the upwind PSD from the downwind PSD. This can be done by determining the mass concentration in each size range on the upwind and downwind filters. This is done by multiplying the cumulative size

distribution of each sampler by the total concentration measured. The net PSD is then calculated by taking the difference between the upwind and downwind samplers. This results in a third particle size distribution that represents an estimation of the source PSD. Figure 16 shows the two PSDs used in this example, along with the third resulting PSD. The resulting PSD that is attributed to the source has an MMD of 15μm and a GSD of 2.1. The result is that 28% of measured TSP is PM_{10}. This is not greatly different from the PSD found by Sweeten et al. (1998).

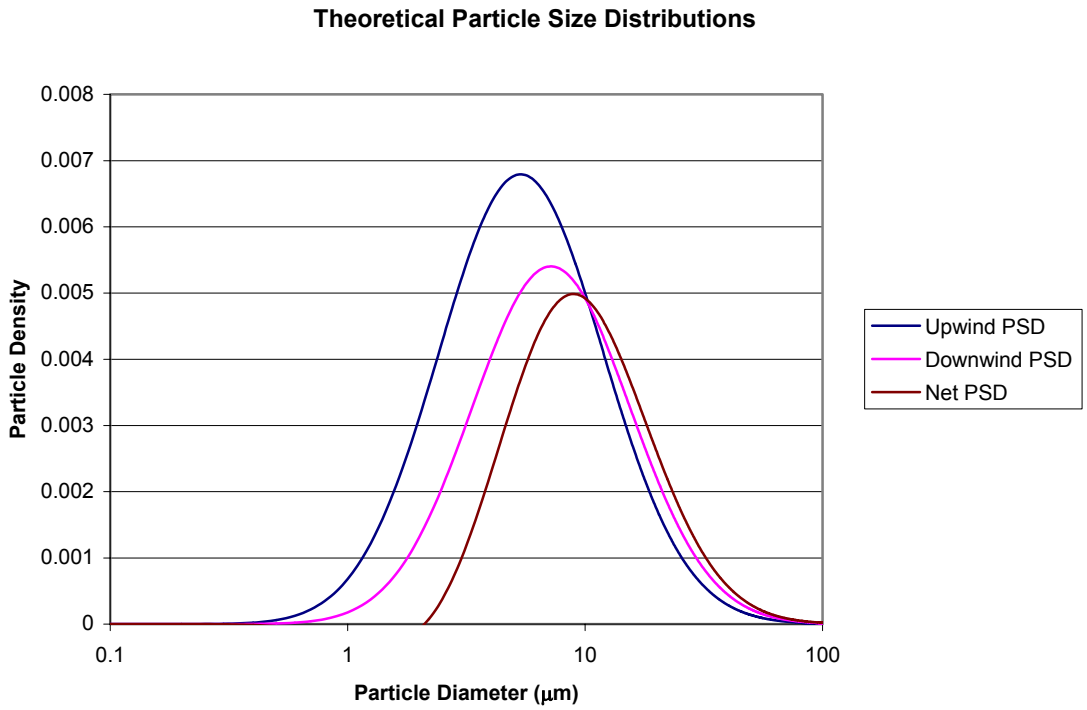

Figure 16. Theoretical upwind, downwind, and net particle distributions.

TSP Emission Rate Calculations

Emission rates are calculated before an emission factor can be determined, due to the differences between the two. Emission factors are a long term estimate of the total emissions from a source category, while the calculated emission rates represent the emissions only during the time of sampling. For example, the emission rates calculated for PM during this study are significantly higher on a per year basis than those that would be calculated from winter sampling, when the soil moisture content is higher from precipitation. There was no significant rainfall for at least 2-weeks before each sampling event, leading to dry soil conditions that are conducive to high PM entrainment by the cattle.

The results of the first sampling period was a grand mean emission rate of 11.9 kg/1000hd/day TSP using the box model. In order to account for the differing activity levels and the resulting variation in emissions throughout the day, each sampling period was assigned to one of four time periods. The day was broken down into 4 time periods of 6 hours each, starting at midnight. The resulting emission rate was calculated as the average of the four time periods. This process prevented the inappropriate weighting of the emission factor for periods that have more samples. The results of time averaging the emission rates are shown in Table 8 for the ICBM. Table 9 shows the temporal distributed emission rates determined using the ICBM. Table 10 shows the emission

rates as determined using ISC-STv3. Table 11 shows the temporal distribution of emission rates developed using ISC-STv3.

The emission rate calculated using ISC-STv3 can be further broken down to identify different emission rates throughout the facility. This is due to the ability to predict the emission contribution from each source using ISC-STv3. For example, receptor 3 with a southern wind will only measure emissions from the open pens; receptor 5 will only measure emissions from the free stalls when there are easterly winds. This allows for a differentiation of emission rates throughout the facility. Table 12 shows the facility apportionment of the emissions, and the resulting emission rate for open pens and free stall areas separately as determined using ISC-STv3. This also shows the drastic difference in emission rates for the two different sources. The free stall areas are paved concrete with minimal possibility for emissions, while the open pens are similar to feed yards with the cattle on a manure pack that is more easily entrained.

Table 8. Calculated emission rates (kg/1000hd/day TSP) for the first sampling season using the ICBM. Cells labeled "--" represent sampling locations with unusable data. Sampler numbers correspond to sampling locations labeled on Figure 15.

	Sampler								Time
Test #	1	2	3	4	5	6	7	8	Period
1	--	--	5.7	--	--	--	--	20.3	2
6	--	--	--	--	--	3.7	--	6.2	2
7	--	--	--	--	--	7.3	--	9.5	3
11	--	--	11.9	--	--	--	--	17.7	2
12	27.9	--	--	--	--	--	12.2	--	3
13	--	--	--	11.8	--	--	16.2	--	3
15	--	--	33.7	--	6.8	--	0.0	--	4
16	--	--	2.8	4.7	--	--	2.7	0.8	1
17	--	--	--	--	2.6	--	--	--	2
18	--	--	--	--	15.6	--	--	--	3
19	--	--	--	--	16.9	--	--	--	3
20	--	--	--	--	37.6	--	--	--	4

Table 9. Time weighted emission rate using the ICBM (kg/1000hd/day TSP).

Time Period	1	2	3	4	Time Weighted Average
	12am-6am	6am-12pm	12pm-6pm	6pm-12am	
Emission Rate	2.7	9.7	15.1	26.0	13.4

Table 10. Calculated emission rates (kg/1000hd/day TSP) for the first sampling season using the ISC-STv3. Cells labeled "--" represent sampling locations with unusable data. Sampler numbers correspond to sampling locations labeled on Figure 15. Bold numbers indicate emissions are attributable to the open pens, and italicized numbers indicate the emission are attributable to free stall areas.

	Sampler								Time
Test #	1	2	3	4	5	6	7	8	Period
1	--	--	**6.2**	--	--	--	--	*19.7*	2
6	--	--	--	--	--	*1.8*	--	*6.0*	2
7	--	--	--	--	--	*7.3*	--	*7.6*	3
11	--	--	**32.7**	--	--	--	--	*15.3*	2
12	**48.3**	--	--	--	--	--	*24.7*	--	3
13	--	--	--	--	--	--	*32.5*	--	3
15	--	--	**56.9**	--	*2.0*	--	--	--	4
16	--	--	**2.7**	**4.7**	--	--	*1.5*	*0.7*	1
17	--	--	--	--	*5.7*	--	--	--	2
18	--	--	--	--	*16.8*	--	--	--	3
19	--	--	--	--	*16.5*	--	--	--	3
20	--	--	--	--	*31.3*	--	--	--	4

Table 11. Time weighted emission rate using ISC-STv3 (kg/1000hd/day TSP).

Time Period	1 12am-6am	2 6am-12pm	3 12pm-6pm	4 6pm-12am	Time Weighted
Emission Rate	2.4	12.5	22.0	30.1	16.7

Table 12. Source apportioned and time allocated emission rates (kg/1000hd/day TSP) for the free stall dairy developed using ISC-STv3.

Time Period	1 12am-6am	2 6am-12pm	3 12pm-6pm	4 6pm-12am	Time Weighted
Free Stall Emission Rate	1.1	9.7	17.6	16.6	11.3
Open Pen Emission Rate	3.7	19.4	48.3	56.9	32.1

Using ISC-STv3 the grand mean emission rate is 16.3 kg/1000hd/day TSP (Table 6). The time weighted average emission rate is 16.7 kg/1000hd/day TSP (Table 7).

The second season of sampling had significantly improved meteorological conditions for field sampling. A significantly higher rate of sample recovery ensued, leading to much higher quality. The number of sampling locations was also decreased in order to more efficiently allocate resources. Only sampler locations 1, 2, 3, 7, and 8 were used during this season. Sampler locations 1 and 2 were always upwind. Table 13 shows the calculated emission rates using the ICBM for each of the three downwind sampling locations. The decrease in the calculated emission rate for the three sampler locations can be attributed to the differences in the actual emission rate of the two main sources on the facility. As the sampler location moves downwind, it is sampling from a larger population of cattle that are in the free stalls, and therefore the emission rate is more representative of cattle in free stalls than cattle in open pens. During this sampling campaign, sampler location 3 was downwind of only the open pens at all times, and therefore only represents emission from that source. Sampler location 7 received

emissions from both the open pen and the free stall directly up wind. Table 14 represents the time weighted emission rate calculated using the ICBM.

Table 13. Calculated emission rates (kg/1000hd/day TSP) for the second sampling season using the ICBM. Sampler numbers correspond to sampling locations labeled on Figure 15.

	Sampler			Time
Test #	3	7	8	Period
2	70.4	N/A	5.3	4
3	39.2	15.0	6.1	1
4	21.7	21.3	4.3	1
5	95.0	87.9	23.9	2
6	48.5	46.0	14.3	3
7	27.9	29.8	37.5	3
8	14.4	26.9	8.0	4
9	40.9	22.4	4.0	1
10	11.6	11.6	5.8	1
11	86.8	29.1	11.8	2
12	23.0	26.5	8.1	3
13	21.5	22.8	6.0	3
14	53.9	19.9	4.0	4
15	1.0	0.5	0.0	1
Average	39.7	27.7	9.9	

Table 14. Time weighted emission rate using the ICBM (kg/1000hd/day TSP) for the second sampling season.

Time Period	1	2	3	4	Time Weighted Average
	12am-6am	6am-12pm	12pm-6pm	6pm-12am	
Emission Rate	13.7	55.7	26.0	25.3	30.2

Table 15 shows the emission rates calculated using the ISC-STv3 for the second sampling season. These emission rates can be compared to Table 13 to observe the differences between ISC-STv3 and the ICBM. Table 16 contains the time weighted emission rates determined with ISC-STv3 for the second sampling season. Table 17

comprises the source apportioned emission rate determined using ISC-STv3. Sampler 3 was attributed to the open pen, and samplers 7 and 8 were attributed to the free stall area.

Table 15. Calculated emission rates (kg/1000hd/day TSP) for the second sampling season using the ISC-STv3. Sampler numbers correspond to sampling locations labeled on Figure 15.

	Sampler			Time
Test #	3	7	8	Period
2	36.3	N/A	6.5	4
3	21.6	9.9	9.2	1
4	15.5	20.8	4.7	1
5	97.7	83.6	41.5	2
6	70.4	50.6	24.6	3
7	39.8	32.9	63.4	3
8	6.9	19.5	12.0	4
9	30.8	18.1	6.1	1
10	9.6	10.6	6.4	1
11	147.5	2.7	14.9	2
12	51.4	30.6	14.6	3
13	33.8	26.3	10.8	3
14	35.4	15.8	6.1	4
15	5.8	1.8	0.0	1
Average	43.0	24.9	15.8	

Table 16. Time weighted emission rate using theISC-STv3 (kg/1000hd/day TSP) for the second sampling season.

Time Period	1	2	3	4	Time Weighted Average
	12am-6am	6am-12pm	12pm-6pm	6pm-12am	
Emission Rate	11.4	64.6	37.4	17.3	32.7

Table 17. Source apportioned and time allocated emission rates (kg/1000hd/day TSP developed using ISC-STv3 for the second sampling season.

Time Period	1	2	3	4	Time Weighted Average
	12am-6am	6am-12pm	12pm-6pm	6pm-12am	
Free Stall Emission Rate	8.7	35.6	31.7	12.0	22.0
Open Pen Emission Rate	16.7	122.6	48.8	26.2	53.6

The resulting emission rate from both sampling seasons is presented in Table 18. This is calculated by compiling all the samples for each time period from each season and source. This represents the total TSP emission rate for each source, not corrected for seasonal variations.

Table 18. Source apportioned temporally averaged TSP emission rate for free-stall dairies for both sampling seasons (kg/1000hd/day).

Time Period	1	2	3	4	Time Weighted
	12am-6am	6am-12pm	12pm-6pm	6pm-12am	
Free Stall Emission Rate	7.5	21.2	25.7	13.3	16.9
Open Pen Emission Rate	13.0	71.0	48.7	33.9	41.6

This TSP emission factor represents a drastic reduction below any of the past emission factors for feed yards and dairies. Even the highest time period average emission rate is significantly less than the yearly average used in the past.

PM_{10} Emission Rate Calculations

The PM_{10} emission rate can be calculated using the ratio of PM_{10} to TSP of 28%. Therefore, the PM_{10} emission rates are 28% of the TSP emission rate. Table 19 shows the time weighted, source apportioned, PM_{10} emission rate from both years of sampling. This represents the maximum possible emissions from the dairy, and is not representative of actual emission during normal operation. It is only representative of operation during summer conditions.

Table 19. Time weighted source apportioned PM_{10} emission rate for the two primary sources on a free stall dairy (kg/1000hd/day).

Time Period	1	2	3	4	Time Weighted Average
	12am-6am	6am-12pm	12pm-6pm	6pm-12am	
Free Stall Emission Rate	2.1	5.9	7.2	3.7	4.7
Open Pen Emission Rate	3.6	19.9	13.6	9.5	11.7

The resulting PM_{10} emission rate is significantly lower than the current emission factor used in California for free stall dairies of 61.2 kg/1000hd/d. This is significant because this emission rate has not been corrected for rainfall events at this point. It should also be noted that the open pen emission rate of 11.7 kg/1000hd/d is close to that published by Parnell et al. (1999) of 8.6kg/1000hd/day for feedyards uncorrected for rainfall events.

For modeling purposes the emission flux uncorrected for rainfall events would be 6.25μg/m^2/s for the free stall and 3.17 μg/m^2/s for the open pens. The higher flux for the free stall emissions is due to the higher stocking density in the free stall structures.

Emission Factor

A final emission factor for two regions that have a large dairy presence is calculated below. Due to the extensive dairy industry in California's San Joaquin Valley combined with the regulatory conditions in the region, a seasonally adjusted emission factor is developed for this region. An emission factor is also developed for the region that the facility was actually located in Central Texas.

Using the number of zero emissions days determined previously for California's San Joaquin Valley, the maximum emission rate can be adjusted downward by 24% to account for rainfall events. This is only applied to the open pen emission rate, due to the fact that rainfall will not directly suppress PM emission from the free stall. This is a conservative estimate based on the assumption that any one rainfall event will not suppress emissions for more than two days. Therefore, the open pen emission rates in table 16 will be reduced by 24% to account for these events. Table 20 shows the final PM_{10} emission factor. This represents the best science available for the development of emission factors from dairies.

Table 20. Time weighted, source apportioned and seasonally corrected annual PM_{10} emission factor for free stall dairies in the San Joaquin Valley (kg/1000hd/day PM_{10}).

Time Period	1 12am-6am	2 6am-12pm	3 12pm-6pm	4 6pm-12am	Time Weighted
Free Stall Emission Rate	2.1	5.9	7.2	3.7	4.7
Open Pen Emission Rate	2.8	15.1	10.4	7.2	8.9

The results in Table 20 represent 2 emission factors for dairies. The free stall emission rate represents the cattle that are kept in free stall structures, while the open pen emission rate represents cattle in open pen configurations. Therefore, if a dairy is all open pens it will have an emission rate of 8.9kg/1000hd/day. Conversely a facility that is strictly free stall will have an emission factor of 4.7 kg/1000hd/day. For facilities that are a combination of the two, the emission rate can be weighted based on herd characteristics.

The resulting flux for modeling purposes is determined by dividing the emission factor by the animal spacing, and converting to the appropriate time units. For California conditions the emission factor in the form of flux for free stalls is 5.9μg/m^2/s, and the flux from the open pens is 2.2μg/m^2/s. The flux number for the open pens is ½ that of the free stall flux due to the animal spacing on the facility.

By using the precipitation correction presented by Parnell et al. (1999) the emission factor for the free stall dairy that sampling was conducted on would be,

4.7kg/1000hd/day PM_{10} for the free stall portion of the dairy and 9.2 kg/1000hd/day PM_{10} for the open pen portion of the dairy. The resulting flux for this case is 5.9μg/m^2/s PM_{10} for the free stalls and 2.5μg/m^2/s PM_{10} for the open lot areas of the facility.

By combining the free stall and open lot emission rates for each region, a total emission factor can be determined for unique facilities for emission inventory purposes. This is done by simply weighting the source specific emission factor by the actual number of head on the facility in the specific housing type. This is done for the facility that sampling was conducted on. Table 21 shows the total emissions for the sampled facility if it were in the San Joaquin Valley and if it were in Texas. The results show that for 1840 cattle in the configuration shown above the total yearly emissions are 3800 kg/year for the San Joaquin Valley and 3900 kg/yr for Texas.

Table 21. Total PM_{10} emissions for the sampled dairy (kg/day) if it was in California's San Joaquin Valley and if it was in Texas.

	Open pen	Free Stall	Total
SJV	4.0	6.5	10.5
Texas	4.2	6.5	10.7

Comparison of ICBM and ISC-STv3 Emission Rates

Chapter III stated that the ICBM will always predict a higher emission flux than ISC-STv3 for a single upwind source that is sufficiently large in the crosswind direction. The

emission rates (emission flux) calculated from the actual field sampling show the opposite results. This is attributable to the differences in the source configuration of the actual facility tested. The ICBM assumes a single uniform source upwind of the sampler location. The facility that sampling was conducted on has multiple sources and is not adequately represented by a single upwind source. Figure 15 shows the configuration of the source on the facility. The ICBM cannot account for this change in source configuration. The ICBM is strictly dependant on upwind source area, not the actual configuration of that source area. For example, the ICBM will predict the same emission rate for an upwind source that is 40 meters deep, as it will for 2 upwind sources that are each 20 meters deep with a 20 meter gap in between. The ICBM assumes that all source area upwind of the sampler contributes equally to the sampler concentration, while ISC-STv3 accounts for the varying upwind distance of a source with the vertical dispersion coefficient.

The variation in the ICBM method, and the inability for the differentiation between upwind sources, make it a poor choice for use in complicated sources. The complicated source configuration contributed to the inability to place samplers in optimum locations (such as center of source on the downwind edge) that would fulfill the assumptions made in the previous chapter. The results of these complications is actually a model that under predicts the emission rate compared to the ISC-STv3 model. This is unacceptable due to the possibility of under predicting the possible exposure of emission to the general public. That is not to say that there are not instances in which it would be a useful tool

for the development of emission rates from some sources. This just highlights the significant importance of examining a method for emission rate development in several circumstances, and not just applying it across the board.

Modeling Ambient Concentrations Around the Dairy

In order to determine the effect of the emission factor on public health, the configuration of the dairy was modeled using ISC-STv3 with 5 years of meteorological data obtained from the Texas Commission on Environmental Quality (TCEQ) (2005). This was done to determine if a buffer zone is necessary to avoid exceeding the NAAQS around a facility that is similar to the one that was used for this study. The meteorological data uses the San Angelo surface station and the Stephenville upper air station. The facility was modeled using the summer emission flux for the years 1985, 1987, 1988, 1989, and 1990. This is the data that the TCEQ would use for permitting purposes.

The facility was entered into ISC-STv3 and a uniform polar grid was used. The grid had its origin in the center of the dairy and extended out 500 meters with 36 radials. The on site receptors were removed. Table 22 shows the results of this modeling for each year. There was not an exceedance of either the 24-hour NAAQS of 150μg/m^3 or the 1 year NAAQS of 50μg/m^3 for any year.

Table 22. Maximum predicted 24-hour and annual concentration (μg/m^3) at a dairy in Central Texas.

Year	24-Hour	Annual
1985	85.2	28.0
1987	72.3	27.2
1988	69.7	26.6
1989	67.1	24.5
1990	70.3	27.9

Conclusions

Ambient TSP concentrations were measured during the summers of 2002 and 2003 on a commercial free stall dairy in central Texas. The facility used both free stall housing structures, as well as open pen housing to accommodate approximately 1840 cattle. The spacing in the open pen was 46.5m^2/hd and the free stall spacing 9.2m^2/hd.

Measurements recorded during the summer of 2002 had an average upwind TSP concentration of 115μg/m^3, with a maximum of 231μg/m^3 and a minimum of 41.4μg/m^3. The net downwind concentrations averaged, 134 μg/m^3, with a maximum of 491μg/m^3 and a minimum of 14μg/m^3. The following summer season the average upwind TSP concentration was 76 μg/m^3, with a maximum measured concentration of 154μg/m^3 and a minimum of 37μg/m^3. The net downwind concentrations averaged 118μg/m^3, with a maximum of 392μg/m^3 and a minimum of 30μg/m^3.

The mean downwind MMD was 12.9 μm corrected to AED with a GSD of 2.23. The mean upwind MMD was 10.1μm corrected to AED with a GSD of 2.16. The downwind

PSD was significantly influenced by the ambient PSD due to the small amount of mass that was collected on the filters. Therefore, the downwind PSD was corrected by using the difference between the upwind and downwind PSD. The resulting PSD that is attributed to the source has an MMD of 15μm and a GSD of 2.1. The result of the particle size distribution is that the PM_{10} fraction of TSP is 28%.

The TSP emission rate calculated by the ICBM did not exceed the emission rate calculated by ISC-STv3 as expected. This is due to the complicated source configuration on a free stall dairy, combined with the non-ideal sampler placement on the facility. The lower emission rate calculated by the ICBM is not a conservative estimate of emissions from the facility, in terms of public safety. Therefore, the results from this analysis would not be accepted by the regulatory community, as would the results from ISC-STv3. Although, the use of the ICBM model, with more simple sources that more closely resemble a single uniform source, still has promise.

The worst case scenario PM_{10} emission rate for the free stall structure was determined to be 4.7 kg/1000hd/day and 11.7kg/1000hd/day for the open pen. This number must be corrected for seasonal variation in order to represent the yearly emission on the facility. It is assumed that the only method of emissions suppression that must be corrected for were rainfall events. An historical account of rainfall events in California's San Joaquin Valley was used, along with historical evapotranspiration numbers, to determine the probable number of days each year that would have no emissions. The results of this

analysis are that approximately 88.5 days each year, or 24% of the time, there will be no emissions. Therefore, the maximum emission rate was reduced by 24% in order to account for the rainfall events in the San Joaquin Valley. This analysis could be done anywhere that historical precipitation and evapotranspiration data is available.

Modeling of the facility using five years of meteorological data shows no exceedences of the NAAQS at the border of the facility. It is likely that most facilities will have a significant buffer zone between the animals and the facility property line resulting in even lower concentrations. This leads to the conclusion that these facilities will not lead to exceedences of the NAAQS at their property lines.

Future Research

There are two primary areas that more research should be pursued. The first area that more research is required would be in expanding the number of facilities sampled. This research was limited to one facility in central Texas. By expanding to other facilities in other areas, a more comprehensive picture of PM_{10} emission from dairies will be obtained. Second, it is necessary to further study the effects of precipitation on PM emissions from ground level area sources. By sampling after precipitation events the duration of suppression could be more accurately determined.

REFERENCES

Algeo, J.W., A. Martinex, C.B. Edam and T. Westing. 1972. *How to Control Feedyard Pollution Bulletin D*. California Cattle Feeders Association, Bakersfield, CA.

Arya, S. P. 1999. *Air Pollution Meteorology and Dispersion*. New York: Oxford University Press, Inc.

ASAE Standards, 46th ed. 1999. EP271.2. Psychrometric Data. St. Joseph, MI: ASAE.

Boriack, C., L.B. Goodrich, and S. Mukhtar, 2003 Revised Design of the Total Suspended Particultate Sampler. 2003 *In Annual Beltwide Cotton Conference*, Nashville, TN.

Buser, M.D., C.B. Parnell, Jr., R.E. Lacey, B.W. Shaw, and B.W. Auvermann. 2001. Inherent Biases of PM10 and PM2.5 Samplers Based on the Interaction of Particle Size and Sampler Performance Characteristics. ASAE Paper no. 01-1167. American Society of Agricultural Engineers; St Joseph, Michigan.

Cooper, C. D. and F.C. Alley. 2002. *Air Pollution Control: A Design Approach.* (3rd ed.) Prospect Heights, IL.: Waveland Press, Inc.

Flocchini, R.G., T.A. James, L.L. Ashbaugh, M.S. Brown, O.F. Carvacho, B.A. Holmen, R.T. Matsumura, K. Trzepla-Nabaglo, and C. Tsubamoto, 2001. INTERIM REPORT. Sources and Sinks of PM_{10} in the San Joaquin Valley. United States Department of Agriculture – Special Research Grants Program. Contract Nos. 94-33825-0383 and 98-38825-6063. August 2001.

Grelinger, M.A. and T. Lapp. 1996. An Evaluation of Published Emission Factors for Cattle Feedlots. *International Conference on Air Pollution from Agricultural Operations.* Midwest Plan Service, Ames, IA.

Haan, C.T., B.J. Barfield, and J.C. Hayes. 1994. *Design Hydrology and Sedimentology for Small Catchments.* San Diego, CA: Academic Press, Inc.

Holzworth, G.C., 1972: Mixing Heights, Wind Speeds and Potential for Urban Air Pollution Throughout the Contiguous United States. Publication No. AP-101, U.S. Environmental Protection Agency, Research Triangle Park, NC.

Houck, J.E., L.C. Pritchett, R.B. Roholt, J.G. Watson, J.C. Chow, J.M. Goulet, and C.A. Frazier, 1989. Determination of Particle Size Distribution and Chemical Composition of Particulate Matter from Selected Sources in California, Final Report. Desert Research Institute & OMNI Environmental. Prepared for California Air Resources Board. Agreement No. A6-175-32.

Meister, M.T. 2000. Air Dispersion Modeling of Particulate Matter from Ground-Level Area Sources. Unpublished Masters Thesis. College Station: Texas A&M University, Department of Agricultural Engineering.

Parnell, C.B., B.W. Shaw, and B.W. Auvermann. 1999. Agricultural Air Quality Fine Particle Project: Task 1 – Livestock Feedlot PM Emission Factors and Emissions Inventory Estimates Final Report. Research sponsored by the Texas Natural Resource Conservation Commission. Department of Agricultural Engineering, Texas A&M University, College Station, TX.

Parnell, S. 1994. Dispersion Modeling for Prediction of Emission Factors for Cattle Feedyards. Unpublished Master of Science Thesis. Department of Agricultural Engineering, Texas A&M University. College Station, TX.

Peters, J.A. and T.R. Blackwood. 1977. Source Assessment: Beef Cattle Feedyards. Report No. EPA-600/2-77-107, EPA, Office of Research and Development, Durham, NC.

Petersen, W.B. and E.D. Rumsey, 1987: User's Guide for PAL 2.0 - A Gaussian-Plume Algorithm for Point, Area, and Line Sources. EPA/600/8-87/009, U.S. Environmental Protection Agency, Research Triangle Park, NC.

Sweeten J.M. and C.B. Parnell. 1989. Particle Size Distribution of Cattle Feedlot Dust. Paper No. 89-4076 Presented at the 1989 International Summer Meeting of the American Society of Agricultural Engineers, Quebec, Canada.

Sweeten J.M., C.B. Parnell, R.R. Etheredge and D. Osborne. 1988. Dust Emissions in Cattle Feedyards. *Veterinary Clinics of North America: Food Animal Products*, 4:(3): 557-578.

Sweeten J.M., C.B. Parnell, B.W. Shaw, and B.W. Auvermann. 1998 Particle Size Distribution of Cattle Feedlot Dust. *Transactions of the ASAE*. Vol. 41(5): 1477-1481.

Texas Commission on Environmental Quality. 2005. Available at http://www.tnrcc.state.tx.us/permitting/airperm/nsr_permits/admt/metsjt.htm. Accessed 21 May, 2003.

Turner, D.B. 1994. *Workbook of Atmospheric Dispersion Estimates: An Introduction to Dispersion Modeling.* (2nd ed.) Boca Raton, Fl: CRC Press, Inc.

Wark, K., C. F. Warner, and W. T. Davis. 1998. *Air Pollution: Its Origin and Control.* (3rd ed.). Menlo Park, CA: Addison-Wesley.

APPENDIX A

APPENDIX A

DISCUSSION ON FEED YARD DRYING TIME AFTER A RAINFALL EVENT

Ambient concentration measurements were made at a feedyard in the pan handle of Texas in the summer of 2002. The same sampling equipment as the dairy was used during this excursion. There were approximately 40,000 cattle at the feed yard and it was laid out in rectangle with the long axis running north south. The prevailing wind was from the south-southwest. There were two samplers placed on the north side of the facility, two sampling location on the west side of the facility and one each on the east and south side of the facility. The south sampling location was placed as the upwind location. This allowed for at least one sampler to always be downwind with varying wind directions. On the second day of sampling, a 10mm rain event occurred that lasted 5 hours. During this period sampling was halted. Immediately after the rainfall event, sampling resumed with the inclusion of a PM_{10} sampler collocated at the N02 sampling location.

The resulting data (Figure A-1) showed a drastic decrease in all measured concentrations due to the suppression of the emission by the rain. The ensuing sampling periods show increasing downwind TSP and PM_{10} concentrations. It also shows an linear increase in the TSP:PM_{10} ratio. This ration indicates a diminishing amount of TSP is PM_{10}. It appears at first glance that the TSP:PM10 ration explains the drying of the facility. However, further analysis shows that the downwind TSP concentrations have not returned to the pre rainfall event levels at the same rate that the TSP:PM10 ratio is returning to the theorized pre rainfall levels. While there were no measurements made of PM_{10} before the rainfall event, it is assumed that the TSP:PM_{10} ration would be approximately 4 (representing 25% of TSP is PM_{10}). The graph shows that after 2 days of drying time the TSP concentrations are still well below the pre rainfall event concentrations, while the TSP:PM10 ratio is 3.6 (~28% of TSP is PM_{10}). This represents a break in the data that must be rectified. The problem simply stated is that the TSP concentrations are not approaching the pre rainfall event levels as quickly as the PM10 TSP ratio is.

In order to rectify the low concentration measurements with the ratio of TSP:PM_{10} there must be another explanation of the ratio of TSP:PM_{10} than simply the drying of the feed yard. The initial TSP:PM10 ratio is indicative of ambient concentrations after rainfall, that the ambient concentration of PM in the air is primarily PM_{10} with little mass represented by particles greater than 10μm. As time passes after the rainfall event, ambient concentrations of PM_{10} gradually increases but not greatly. The ambient PM concentrations are expected to consist of only PM_{10} representing a TSP:PM_{10} ratio equal to 1. This represents a constant increase in the measured PM10 (and TSP) downwind of the facility. (Assuming all upwind TSP is PM10, a 1:1 ration can be applied to this source of PM) Now, lets assume that the feed yard surface dries in such a way as to emit particulate matter with constant TSP:PM10 ratio. That is to say, contribution at the

downwind sampler of TSP and PM10 from the feedyard is a constant ratio of 25% (Using the measured ratio of TSP:PM10) What we observe is initially an increasing ratio of TSP:PM10 just as the graph shows with an eventual asymptotic approach to the TSP:PM10 ratio of feedyard PM emissions. This also shows that the TSP:PM10 ratio will approach ~25% much sooner than the downwind TSP measured concentration reaches the pre rainfall levels. This is due to the diminishing proportion of ambient particulate matter on the downwind sampler compared to source particulate matter. The final result of this analysis is that there is a possibility of significant dust suppression due to the moisture in the manure pack surface that is not reflected in the TSP:PM10 ratio but is reflected in the increase in measured TSP concentration.

This also shows that although the TSP:PM_{10} ratio has approached 4, the dust suppression of the rainfall event continues. Therefore, the best indicator of feed yard drying is the downwind concentration measurement and not the TSP:PM_{10} ratio.

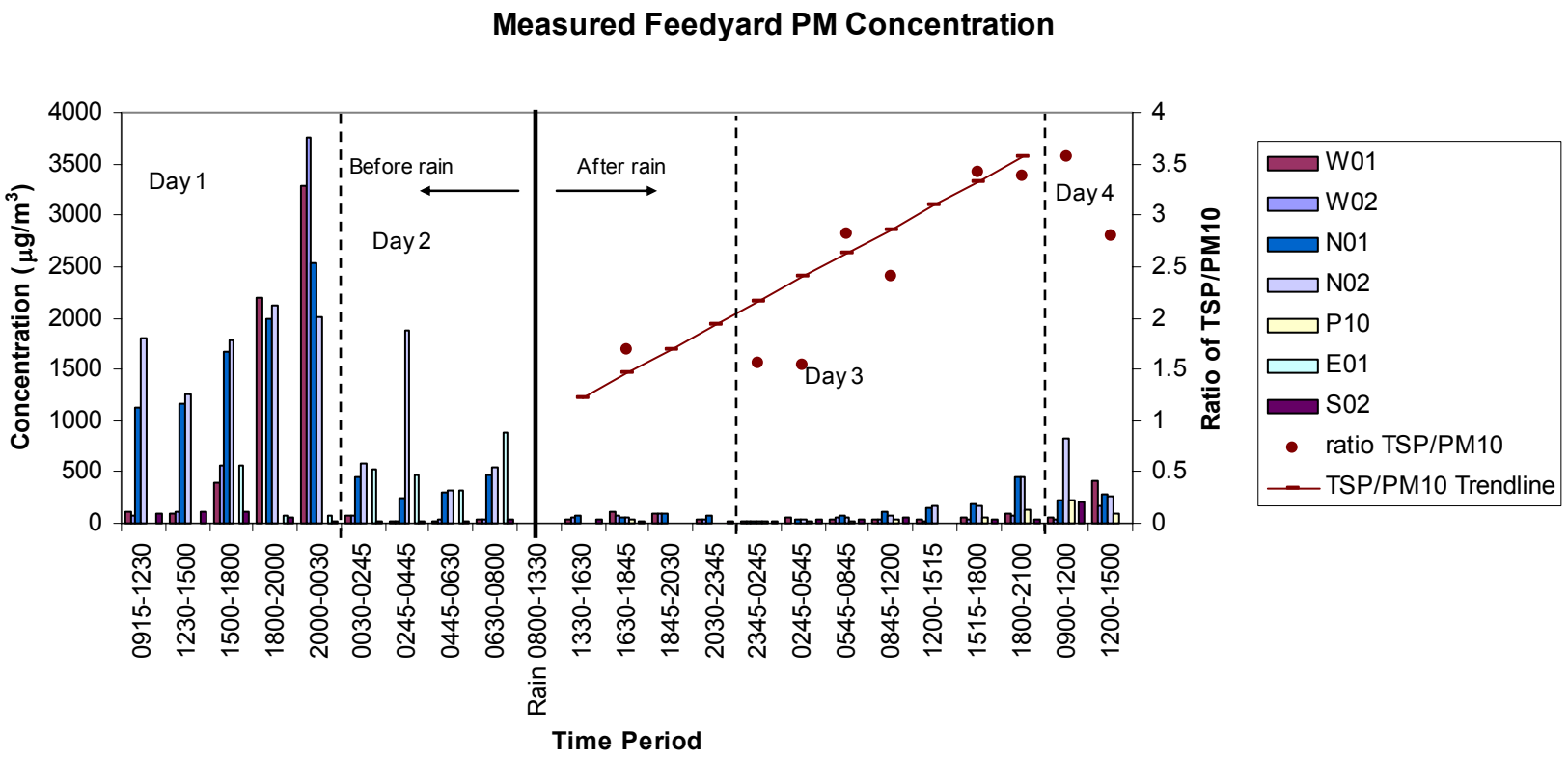

Figure A-1. Concentration and TSP:PM10 ratio at a feed yard in the summer of 2002

VITA

Lee Barry Goodrich

Education

Master of Science. May 2006. Department of Biological and Agricultural Engineering. Texas A&M University
Emphasis: Agricultural Air Quality Engineering and Science

Bachelor of Science. May 2001. Department of Biological and Agricultural Engineering. Texas A&M University

Correspondence can be sent to

Department of Biological and Agricultural Engineering, Texas A&M University College Station , TX 77843-2117

Papers and Presentations

Boriack, C., L.B. Goodrich, S. Mukhtar. 2003. Revised Design of the Total Suspended Particultate Sampler. *Proceedings of the 2003 Annual Beltwide Cotton Conference*. Nashville, TN

Goodrich, L.B., C.B. Parnell Jr., S. Mukhtar, B.W. Shaw, and R.E. Lacey. 2004. Preliminary PM_{10} Emission Factor for Free Stall Dairies. *Proceedings of the 2004 International Emission Inventory Conference* Las Vegas, NV

Goodrich, L.B. C.B. Parnell Jr., S. Mukhtar, B.W. Shaw, and R.E. Lacey. 2003. Evaluation of the Use of the Box Model to Determine Emission Fluxes from Area Sources and the Corresponding Modeled Concentrations Using the Industrial Source Complex. *Proceedings of the 2003 Annual Beltwide Cotton Conference.* Nashville, TN

Goodrich, L.B. C.B. Parnell Jr., S. Mukhtar, B.W. Shaw, and R.E. Lacey. 2003. A Science Based PM_{10} Emission Factor for Free Stall Dairies. *Proceedings of the 2003 Annual International Meeting of the American Society of Agricultural Engineers.* Las Vegas, NV, Paper No. 034115

Goodrich, L.B. C.B. Parnell Jr., S. Mukhtar, B.W. Shaw, and R.E. Lacey. 2002. A Preliminary PM_{10} Emission Factor for Free Stall Dairies. *Proceedings of the 2002 Annual International Meeting of the American Society of Agricultural Engineers.* Chicago,IL Paper No. 024214